Structural inheritance in the Central Pyrenees: the Variscan to Alpine tectonometamorphic evolution of the Axial Zone

Bryan Cochelin, Baptiste Lemirre, Yoann Denèle, Michel de Saint Blanquat, Abdeltif Lahfid, Stéphanie Duchêne

Structural inheritance in the Central Pyrenees: The Variscan to Alpine tectono- metamorphic evolution of the Axial Zone

Bryan COCHELIN [a,b] *, Baptiste LEMIRRE[a], Yoann DENELE[a], Michel de SAINT BLANQUAT[a], Abdeltif LAHFID [b], Stéphanie DUCHENE [a]

[a] Géosciences Environnement Toulouse, Université de Toulouse, CNRS, IRD, UPS, CNES, F-31400, France

[b] BRGM, 3 avenue Claude Guillemin, F-45060 Orléans, France

* corresponding author: bryan.cochelin.get@gmail.com

Submitted to *Journal of the Geological Society*, 24 May 2017

Revised, 05 September 2017

Abstract

Estimating structural inheritance in orogens is critical to understand the manner in which plate convergence is accomodated. The Pyrenean belt, which developed in Late Cretaceous to Paleogene times, was affected by Cretaceous rifting and Variscan orogeny. Here we combine a structural and petrological study of the Axial Zone in the Central Pyrenees to discuss structural inheritance. Low-grade Paleozoic metasedimentary rocks were affected by a Variscan transpressional event that produced successively: (i) regional-scale folds; (ii) isoclinal folding, steep pervasive cleavage and vertical stretching, synchronous with peak metamorphism; (iii) and strain localization into ductile reverse shear zones. The persistence of a relative flat envelop for the Paleozoic sedimentary pile and Variscan isograds, and the absence of Alpine crustal-scale faults in the core of the Axial Zone, suggest that the Axial Zone constitutes a large Variscan structural unit preserved during Pyrenean orogeny. This configuration seems to be inherited from Cretaceous rifting, which led to the individualization of a large continental block (future Axial Zone) against a hyper-extended domain along the North Pyrenean Fault zone. This study places the currently prevailing model of Pyrenean belt deformation in a new perspective and bears important implications for crustal evolution and inheritance in mountain belts more generally.

Keywords: Structural inheritance, Pyrenean belt, Variscan orogeny, Passive margin inversion, Central Pyrenees, RSCM thermometry

Supplementary materials:

- Table with RSCM data. - Figure illustrating peak-fitting of the Raman spectrum of carbonaceous material and Raman spectra from the various samples of the Pallaresa cross-section

The crustal architecture of a mountain belt narrowly depends on the rheology and relative thickness of the continental plates involved in the collision. If the two plates were passive margins, both were affected by rifting before convergence, leading to variably thinned domains of continental crust, dismembered by normal faults or detachments. At the initiation of convergence, the thickness and structure of the two margins exert first-order controls on the architecture of the mountain belt (Mouthereau & Lacombe, 2006; Wrobel-Daveau et al., 2010; Mohn et al., 2012; Mouthereau et al., 2012; McIntosh et al., 2013; Masini et al., 2014; Bellahsen et al., 2014). The thinnest and thermally weaker continental margin is preferentially affected by shortening during inversion of the rift systems and favourably orientated structures, which are inherited from rifting, could be reactivated (Beaumont et al., 2000; Masini et al., 2011; Mouthereau et al., 2012, 2013; Mesalles et al., 2014; Vacherat et al., 2014). At the paroxysm of collision, when the two margins are accreted into the orogenic prism, new thrusts (unrelated to the rift) are generated to balance shortening, and pre-rift structures within the basement may undergo reactivation (Cloke et al., 1997; Allen et al., 1998; Soulaimani & Burkhard, 2008). However, the importance of these long-term inherited structures is most of the time overlooked because of the polyphase tectonic history or because of the absence of structural markers to constrain it.

The importance of rift-related structures has been previously illustrated in the Pyrenees (Choukroune, 1992), where the European and Iberian plates began to collide in Late Cretaceous times (Dubois & Seguin, 1978; Roest & Srivastava, 1991; Olivet, 1996). Early Cretaceous rifting led to the formation of an ultra-thinned northern margin and to the exhumation of subcontinental mantle (Lagabrielle and Bodinier, 2008; Lagabrielle et al., 2010; Masini et al., 2014; Clerc & Lagabrielle, 2014; de Saint Blanquat et al., 2016; Vacherat et al., 2016). While the European margin was hyper-extended in Cretaceous times, no evidence of this type of extension has been detected in the Iberian plate, i.e. in the hinterland and in the southern foreland of the Pyrenean

belt. This hinterland, which corresponds to the so-called Axial Zone, is mainly made of Paleozoic metasediments and magmatic bodies involved in the Variscan orogeny (Fig. 1a & 1b). Deep exhumation of the Axial Zone is responsible for the erosion of post-Variscan deposits, which form the main structural marker of the Cretaceous rifting event and Pyrenean collision. Since the ECORS deep seismic profile (Roure et al., 1989; Choukroune, 1989; Choukroune et al., 1990), the Pyrenees were interpreted as an asymmetric, doubly vergent collisional wedge with numerous stacked crustal units in the Axial Zone (Fig. 1c). Whereas this geometry is in agreement with structural observations made in the Central to Western Pyrenees, where the crustal-scale north-dipping Gavarnie and Les Eaux Chaudes/Lakhora thrusts are observed (Fig. 1b), the continuity of these structures in the Central and Eastern Pyrenees has remained debated (Carreras and Debat, 1996; Soler et al. 1998; Laumonier, 2015). Moreover, the anticlinal nappe-stack model developed by Muñoz (1992) implies that the Variscan crust of the Central Pyrenees was deeply affected by both Cretaceous rifting and Alpine orogeny, implying large-scale bloc rotations, internal deformation and thrusting (Berastegui et al., 1993; Beaumont et al., 2000; Mouthereau et al., 2014). Nevertheless, detailed structural studies performed at local scale on the Variscan crust in the last 20 years tend to indicate only limited reactivation of Variscan structures (Bons, 1988; Carreras & Debat, 1996; Capella and Carreras, 1996; Soler et al., 1998; Mezger & Passchier, 2003; Denèle et al. 2008; Clariana & García-Sansegundo, 2009; Laumonier, 2015).

In order to resolve this apparent paradox, we try here to better constrain the deformation of the Central Pyrenees through time. We combine a structural, petrological and geothermometric study of the Variscan crust along the ECORS seismic profile. This study allows us to discuss the structure of the hinterland of the central Pyrenean belt and the relative impact of structures inherited from the Lower Cretaceous rifting event and from the Variscan orogeny. We also propose a new model of the eastern Pyrenean crustal wedge in which a pop-up structure corresponding to the Axial Zone was thrusted over the southern foreland along moderately

dipping ramps. This constitutes an alternative view by comparison to the currently prevailing model (Muñoz et al., 1992), which advocates severals steeply-dipping thrusts cross-cutting the Axial Zone.

Geological setting

The Axial Zone of the Pyrenean range is classically described as being affected by thick-skinned tectonics involving several basement thrust sheets (Fig. 1c), namely the Lakhora, Gavarnie and Bielsa units in the western part (Teixell et al., 1998), and the Nogueres, Orri, and Rialp units in the east (e.g. Vergés et al., 1995). The crustal-scale, north-dipping Gavarnie and Les Eaux Chaudes/Lakhora thrusts that placed basement rocks over Cretaceous cover constitute a major feature of the Pyrenean range and have been studied in detail. In the field, these two thrusts form hundred metre-thick high-strain zones, mainly consisting of brittle–ductile mylonites and breccia (Déramond, 1979; Majesté-Menjoulas, 1979). The Nogueres unit (Fig. 1c) is defined in the northern part of the Axial Zone (Muñoz, 1992) as the rooting zone of the so-called "têtes plongeantes" or "plunging noses" defined to the south of the Axial Zone, that consists of overturned synforms of Devonian to Permo-Triassic series (Vergely, 1970; Séguret, 1972; Choukroune & Séguret, 1973). This basement sheet is interpreted as the lateral continuity of the Gavarnie unit separated from the Orri unit to the south by the Gavarnie thrust (Beaumont et al., 2000; Mouthereau et al., 2014). While this thrust is clearly identified in the western Axial Zone (Majesté-Menjoulas, 1979), its lateral continuity in the Central Pyrenees is discussed, as this zone is devoid of post-Variscan deposits to identified Pyrenean thrusting, except one outcrop of Triassic deposits, deformed in a fault zone located north on the Maladeta massif (Fig. 2 & 3, see Soler et al., 1998).

The Axial Zone consists of Precambrian and Paleozoic rocks that were affected by the Variscan orogeny between 330 Ma and 290 Ma (Denèle et al., 2014 and references therein). The

Variscan orogeny is marked by Permo-Carboniferous deformation, high temperature–low pressure (HT–LP) regional metamorphism, and calc-alkaline plutonism. The Variscan crust of the Axial Zone is classically interpreted as being formed by two contrasting structural levels (de Sitter & Zwart, 1962; Carreras & Capella, 1994): (i) an upper crustal level, also called "Superstructure", made of low-grade metamorphosed Paleozoic sediments and defined by tight to upright folds and steep axial-plane cleavage; (ii) a lower crustal level, or "Infrastructure", mostly characterized by Precambrian to Lower Paleozoic rocks affected by HT–LP metamorphism and exposed into domal structures with shallow-dipping foliation planes. Recent studies suggest that the formation of these two domains was coeval and occurred in a dextral transpressive regime (Gleizes et al., 1998b; Mezger, 2009; Denèle et al., 2014).

In the Central Pyrenees, rocks affected by the Variscan orogeny are made of Cambrian to Carboniferous metasedimentary rocks (Fig. 2). Cambrian to Ordovician rocks occupy the central part of two regional-scale antiforms, the Pallaresa and Orri anticlines (Fig. 2). Whereas the stratigraphy of Cambrian to Lower Ordovician rocks remains poorly constrained because of its azoic character, the stratigraphic continuity between Upper Ordovician conglomerates and lower series in the southern flank of the Pallaresa anticline seems to confirm that the older rocks occupy the core of the anticline (Zandvliet, 1960; Hartevelt, 1970; Laumonier et al., 1996). The lower terms are made of sandstone, locally microconglomerate and limestone at the top, described as belonging to the Cambrian Evol Formation (Laumonier et al., 1996). The upper series, belonging to the Cambrian Jujols Formation (Laumonier et al., 1996), is mainly made of sandstone and greenish to dark schist. The upper Paleozoic series outcrops occur in the Couflens syncline, bording the North Pyrenean Fault, and in the Llavorsi syncline, pinched between the Pallaresa and Orri anticlines (Fig. 2). These Upper Paleozoic rocks are made of (i) thin levels of Silurian black shale and limestone; (ii) a succession of Devonian sandstone, limestone and schist

with significant local variations of facies (see García-Sansegundo et al., 2011 and references therein); and (iii) Middle Carboniferous flysch.

The Cambrian to Paleozoic metasedimentary rocks of the Central Pyrenees are affected by multi-scale folds and pervasive axial-plane cleavage, developed under low-grade metamorphic conditions (Zwart, 1979; Bons, 1988; Capella and Carreras, 1996). The Paleozoic metasedimentary rocks of the Superstructure are intruded by voluminous calc-alkaline plutons such as the Maladeta pluton in the west, the Bassiès, Marimanha and Ribérot plutons in the north, with U/Pb ages ranging between 312 and 298 Ma (Evans, 1993; Paquette et al., 1997; Denèle et al., 2014). The intrusion of these plutons is considered as coeval with the late Carboniferous dextral transpressional event (Bouchez & Gleizes, 1995; Evans et al., 1997; Gleizes et al., 1998a). The Infrastructure marked by HT–LP metamorphic rocks and flat-lying foliations can be observed in the Aston gneiss dome directly to the east of the Pallaresa anticline (Fig. 2) (Mezger, 2009; Denèle et al., 2009).

The central part of the Axial Zone is cut by several shear zones and faults generally considered as Variscan in age, with reactivation during the Pyrenean collision. However, no real consensus exists about the age and relative importance of activation and reactivation of these various faults (Figs. 2 & 3). The older one is the Port de Salau fault, an east–west steeply north-dipping fault. In its current position, its footwall consists of Cambrian rocks belonging to the Pallaresa anticline, and its hangingwall of Siluro-Devonian rocks (Fig. 2). This fault seems to be folded by the late Variscan transpressional event, and is interpreted by some authors as an early Variscan thrust with a probable southward displacement (Bodin and Ledru, 1986; Losantos et al., 1986). Farther south the Lladorre shear zone, localized in Cambrian limestones, is considered by Capella & Carreras (1996) as a late reverse Variscan shear zone. This shear zone constitutes the western continuity of the Variscan kilometre-scale Mérens shear zone (Fig. 2), which was reactivated during the Alpine orogeny as a localized fault (McCaig, 1986; Denèle et al., 2008;

Mezger et al., 2012). Other authors (Berastegui et al., 1993; Beaumont et al., 2000; Vissers & Meijer, 2012) consider this shear zone as an Alpine thrust that could be a hypothetical candidate for the lateral continuity of the Gavarnie thrust, and renamed it the Pallaresa thrust. It is supposed to be responsible for the stacking of the Nogueres sheet over the Orri sheet, with a proposed displacement around 15–20 km. Farther south, the Estarón thrust was considered by Casas et al., (1989) to represent a Variscan thrust, while other authors consider it as another candidate for the continuity to the east of the main Alpine Gavarnie thrust (Metcalf et al., 2009; Mouthereau et al., 2014). Similarly, the Llavorsi thrust is considered to be a Variscan thrust in some studies (Casas et al., 1989; Clariana, 2001), but an Alpine thrust belonging to the Orri sheet in others studies (Zwart, 1986; Vergés et al., 1995, 2002). Its subtractive character, placing Devonian over Cambro-Ordovician rocks, has led some authors to consider it as a normal fault, either Early Carboniferous (Capellà & Bou, 1997), or Late Carboniferous to Cretaceous in age (Casas et al., 2007). Further south, the Orri and Nogueres thrusts are indisputably Alpine in age, putting Paleozoic rocks on Permian to Triassic sediments (Fig. 2). The Orri thrust accommodated 10–15 km of displacement during the collision (Séguret, 1972; Berastegui et al., 1993; Beaumont et al., 2000; Mouthereau et al., 2014) and is supposed to be a reactivated Cretaceous normal fault (Berastegui et al., 1993; Beaumont et al., 2000).

Discussion about the age of shear zones and faults in the Axial Zone of the Pyrenees is due to the scarcity of post-Variscan markers. Syn-kinematic mica in some ductile shear zones has been tentatively dated using $^{40}Ar/^{39}Ar$ methods and provided ages ranging between the Eocene and the Jurassic (e.g. McCaig & Miller, 1986; Monié et al., 1994; Wayne & McCaig, 1998; Vissers et al., 2017). Eocene ages suggest a partial Pyrenean reactivation of some shear zones, as for instance in the Néouvielle massif (Wayne & McCaig, 1998). Nevertheless, $^{40}Ar/^{39}Ar$ ages on mica cannot be readily used as proxies for the absolute age of faults or shear zones. The closure temperature of the Ar/Ar system in mica is around 300 °C (Harrison et al.,

1985), but the Jurassic to Cretaceous ages in Pyrenean shear zones suggest a partial to total rejuvenation of argon isotopic systems during the widespread hydrothermal events ($250 < T < 550$ °C) that occurred between Permian and Cretaceous times (Boulvais et al., 2007; Poujol et al., 2010; Fallourd et al., 2014; Boutin et al., 2016, Boutin, 2016). The difficulties linked to interpreting $^{40}Ar/^{39}Ar$ ages in the Pyrenees have been emphasized by Jolivet et al. (2007), Maurel et al. (2008) and Metcalf et al. (2009), who recognized the effects of the Mesozoic hydrothermal events in the syn-kinematic micas of the Variscan Maladeta and Néouvielle plutons, and in the Canigou massif.

Methodology

Measurement and sampling

This study is based on 330 sites distributed along N–S cross-sections, following the main valleys of the mountains belt (Fig. 2). In order to reconstruct the large-scale geometry of folds, planar and linear strain fabrics and kinematic criteria affecting metasedimentary rocks were systematically measured, as well as the relationship of planar fabric with original bedding. All these measurements are synthesized in Figs. 3 and 4.

Nineteen samples were collected along the Pallaresa cross-section. They were selected in the whole metasedimentary sequence from Cambrian to Devonian (Fig. 2, red dots). At least two samples were collected in each structural domain of the cross-section. Dark-coloured samples rich in organic matter were favoured for Raman Spectroscopy of Carbonaceous Materials (RSCM).

Polished thin sections were prepared normal to the schistosity and parallel to the lineation (XZ planes) for petrographic and microstructural observation.

Raman Spectroscopy of Carbonaceous Materials (RSCM)

Raman Spectroscopy of Carbonaceous Material (RSCM) method is used to estimate the maximum temperature (up to 650 °C) recorded by the metasediments during metamorphism (Beyssac et al., 2002; Lahfid et al., 2010). Delchini et al. (2016) confirmed the applicability of RSCM for studying domains with polyphased metamorphic histories, such as the Pyrenees. Raman analyses were performed at the BRGM, Orléans, using a Ranishaw inVia Reflex system with argon-ion laser source excitation of 514.5 nm. The laser beam is focussed on the sample through a Leica DM2500 microscope specially adapted for the system using a x100 lens, with power of around 0.5 mW at the surface of the thin section. Before each measurement session, the spectrometer was calibrated using the 520.5 cm^{-1} line of a silicon standard. The signal obtained after elimination of Rayleigh diffusion using Edge filters was dispersed using 1800 $lines.mm^{-1}$ grating before being analyzed by a deep depletion CCD detector (1024 x 256 pixels). About 1520 Raman spectra of particles were recorded to check data consistency. Raman parameters, peak temperatures obtained by RSCM and Raman spectra are provided in the Data Repository.

Structures and kinematics

In the study area we observed two types of schistosity. The first generation is penetrative, observed in all Variscan rocks, and called hereafter S1. The second generation is only locally observed and corresponds to a crenulation cleavage. To the south of the Axial Zone, the Cambrian series belonging to the Orri anticline are unconformably overlapped by undeformed Permian and Triassic red beds that crosscut the S1 cleavage (Fig. 5a). These observations attest, in accordance with previous studies (e.g. Zandvliet, 1960; Mey, 1968; Lucas, 1985; Zwart, 1986; Bichot, 1986; Carreras & Debat, 1996) that the regional penetrative cleavage S1 is Variscan in age. By contrast, a discrete crenulation cleavage is observed in Permian and Triassic pelitic levels suggesting that

the second schistosity in the basement units could be Alpine in age (Izquierdo-Llavall et al., 2013). It is hereafter named Sa.

As a first approximation, the Central Pyrenees area is defined by two large and open antiforms forming the Pallaresa and Orri anticlines and the southward verging and pinched Llavorsi syncline (Fig. 3a). The flat attitude of bedding in anticline cores is perturbed by multiscale open to isoclinal folds (Fig. 4) associated with pervasive axial-plane cleavage (i.e. S1; Fig. 5b & b'). S1 shows a homogeneous N95–110E direction (Fig. 3b) with trajectories roughly parallel to the Lladorre–Mérens, Estarón and Llavorsi mylonitic shear zones (Fig. 3a). In the northern half of the Axial Zone, S1 is vertical and dips around 50–60°N in the southern part, excepted 5 km to the north to the Nogueres Unit, where it is subhorizontal or displays shallow dips to the north (Figs 3a & 4). S1 bears steeply-plunging stretching lineations with a homogeneous N150–160° orientation (Figs 3a & 3c).

Structural studies have highlighted three domains of deformation limited by the Lladorre–Mérens and Llavorsi mylonitic shear zones. The northern domain is characterized by a vertical cleavage S1 and an apparent heterogeneous deformation, with highly transposed Devonian to Cambrian limestone and schist and gently folded thick Cambrian microconglomerate and sandstone. This domain is affected by an apparent coaxial deformation attested by the coexistence of "north-side up" and "south-side up" shear criteria on subvertical shear planes. This domain is limited to the south by the 200-m-thick mylonitic shear zone of Lladorre, localized in interbedded sandstones and marbles showing non-coaxial "north-side up" kinematics (Figs 3a, 4 & 5c). The central domain is mostly characterized by the complete transposition of original bedding and associated non-coaxial "top-to-the-south" shear bands (Fig. 5d). This high strain domain corresponds to the southern overturned limb of the Pallaresa anticline and to the pinched Llavorsi syncline, with apparent strain localization in the highly

laminated Silurian black shales. The southern domain, which corresponds to the Orri anticline, is poorly deformed, marked by discrete S1 cleavage oblique to the original bedding. Few discrete C' shears with non-coaxial "top-to-the-south" kinematics were observed, as previously described by Mey (1968).

The S1 trajectories are locally disturbed in the contact aureole of plutons where asymmetric schistosity triple points can be defined (Fig. 3a). Stretching lineations are subhorizontal in these domains, with C' shear bands showing dextral senses of movement (Fig. 6a). Shear bands strike between N100–N130°E and concentrate in narrow mylonitic corridors such as the western part of the Estarón thrust, between the Maladeta and Marimanha plutons (Fig. 3a), or around the Bassiès pluton (Fig. 4).

Over the entire area, the Paleozoic basement is locally affected by late Alpine deformation, mainly localized within 1- to 100-m-thick corridors (Fig. 4). In such corridors, new 0.1- to 1-m-scale folds (Fa), with N80°- to N140°-striking fold axes, affect previously schistose rocks forming kink-bands and chevron folds (Figs. 3b & 3c and 6b & 6c). Crenulation cleavage Sa is common in such corridors. This crenulation cleavage, axial plane of late folds, is sub-vertical in the northern third part of the Axial Zone, striking at a low angle to the regional schistosity S1. In the central part of the Axial Zone, Sa dips steeply to the south (Fig. 6b) and can be easily distinguished from S1, which dips northward (Fig. 4, between Lladorre and Llavorsi). In the southern domain, which corresponds to the Orri anticline, the late crenulation cleavage dips at low angles to the north but seems to be less conspicuous than elsewhere (Fig. 4). Away from these corridors, only a subhorizontal east–west discrete crenulation lineation affects the regional structures. Evidence of brittle deformation is otherwise scarce in the Pallaresa cross-section. Some fault zones have been observed in the Silurian black shales of the pinched Llavorsi syncline. These faults are associated with reverse drags that affect the regional penetrative structures over distances of ~20 m.

Petrological study

Raman Spectroscopy of Carbonaceous Materials (RSCM)

The Raman spectroscopy results are synthesized in Fig. 7. Palaeotemperatures range between 350 °C and 550 °C with a temperature around 350 °C in the Couflens syncline, the Llavorsi syncline and the Orri anticline and an increase up to 550 °C in the Pallaresa anticline. Two significant steps of around 50 °C and 100 °C were observed in the vicinity of the Estarón thrust and the Lladorre shear zone, respectively (Fig. 7a). Isotherms were deduced from the Raman temperature (Fig. 7a). Small steps of maximum 30 °C were evidenced in the Couflens syncline, but these variations cannot be considered as significant in regard of the analytical error on the measurements.

Metamorphic parageneses and microstructures

The optical analysis of the thin sections allowed us to determine the metamorphic parageneses and microstructures and to gain insights into the thermal conditions of deformation in addition to RSCM results. The Devonian sequence in the north (16BL44, 16BL47, 16BL51, 16BL55, 16BL59), close to the NPF, corresponds to limestone with pelitic intercalations. Silurian deposits that belong to the Couflens syncline are dark schists rich in carbonaceous materials (16BL60, 16BL52, 16BL53), with few small chlorite crystals. The northermost Cambrian samples consist of an alternation of thin pelitic and carbonate levels (16BL56) and quartzo-pelitic schist (TP442). The following two samples of the Pallaresa anticline (15BL104, 15BL106) correspond to quartz-rich schist with Ms-Bt-Pl-Qtz (see Kretz, 1983 for the mineral abbreviations). Biotite porphyroblasts have grown parallel to S1. Quartz-rich levels show well-developed dynamic recristallization controlled by grain boundary migrations, attested by a pinning effect on the migrating boundaries (Fig. 8a, Song and Ree, 2007). These types of microstructure and the observation of secondary biotites in schistosity planes suggest a temperature close to 500 °C during deformation (Hirth and Tullis, 1992; Stipp et al., 2002). Such a temperature is consistent with the

apparition of biotite and the absence of andalusite, cordierite and staurolite, which appear above a temperature of 550–600 °C in the pseudosections obtained for similar protoliths from the western Aston dome termination (Mezger & Régnier, 2016) and the Albères massif (Vilà et al., 2007). Within the Lladorre shear zone (samples 15BL110 & 15BL112), well-preserved quartz veins in mylonitic marble show dynamic recrystallization of quartz with an association of sub-grain rotation and grain boundary migration. The transition between these two mechanisms suggests a temperature of deformation at about 500–550 °C (Stipp et al., 2002). A sheared conglomerate that belongs to the upper Ordovician of the southern overturned limb of the Pallaresa antiform and located within the Estarón shear zone (sample 15BL118, Fig. 5d) is composed of Ms-Pl-Qtz±Chl matrix and clasts of quartz. Here, S1 and shear bands are underlined by muscovite (Fig. 8b). Quartz grains show evidence of recrystallization by bulging and sub-grain rotation (Fig 8c & d). Conglomerates show a core and mantle microstructure with grain-size of quartz blasts of about 20 to 50 µm, suggesting a recrystallization temperature of about 400 °C (Stipp et al., 2002). Finally, the two southernmost samples (15BL125, 15BL127) are Cambrian schists from the Orri anticline, with muscovite and chlorite growing parallel to S1 (Fig. 8e).

The evolution from biotite-bearing schist in the Pallaresa anticline to chlorite-bearing schist in Orri anticline, in addition to the quartz recrystallization dynamics, indicate a decrease in palaeotemperature towards the south, which is in good agreement with RSCM results. All along the cross-section, the second cleavage Sa is characterized by microfolds, forming microlithons that affect S1 (Fig. 8e). The development of Sa implies the progressive destruction of previous fabrics by pressure solution, mainly removing quartz grains while phyllosilicates show internal deformation like folding and rotation. In agreement with previous work (Zwart, 1986; Bons, 1988; Soler et al., 1998; Clariana et al., 2008, among others), our observations confirm that Alpine structures in Central Pyrenees were produced under low temperatures, which never reached those obtained during the Variscan orogeny

Relationship between deformation and metamorphism

Given that greenschist and amphibolite facies metamorphic minerals grew within shear planes and underline the main schistosity plane S1, our petrological study highlights that HT–LP metamorphism was synchronous with pervasive deformation. We determined the geometry of the palaeo-isotherms based on the following constraints. The isotherms match the temperatures retrieved from Raman spectroscopy (Fig. 7a). They also account for the absence of abrupt petrological transitions across the section, with regular transitions from greenschist to amphibolite facies assemblage. The isotherms are drawn parallel to each other. They match the geothermal gradient previously estimated in the envelope of the Aston, Albères, Bossost and Canigou gneiss domes (40 to 70 °C/km) (Mezger, 2005; Triboulet et al., 2005; Vilà et al., 2007; Mezger & Régnier, 2016). We end up with a picture of relatively flat isotherms that define a palaeogeothermal gradient of 45 °C/km (Fig. 7b).

On the cross-section in Fig. 7b, isotherms are secant on large-scale folds, such as the Llavorsi syncline. This first-order observation allows us to interpret the metamorphism as subsequent to the initiation of regional-scale folding. Besides, isotherms are vertically shifted by the Lladore and Estarón amphibolite to greenschist facies reverse shear zones, suggesting that shear zone activity ends after peak metamorphism. Our results show (i) that shear zones and regional cleavage form a single and continuous fabric that simply illustrates the strain gradient in the crust; (ii) that mylonites within the shear zones and rocks affected by the regional cleavage exhibit the same amphibolite to greenschist metamorphic parageneses; and (iii) that the regional fabrics and shear zone share the same structural character, with down-dip stretching lineations and dip-slip/reverse sense of shear. Based on this evidence, we consider these shear zones as Variscan in age. They formed during the same tectonic episode as the other regional structures. Because the Lladorre and Estarón amphibolite to greenschist facies reverse shear zones shift the isotherms (Fig. 7b), we propose that their final activity occurred after peak metamorphism and represents the final

expression of the main Variscan deformation recorded in Pyrenees (see discussion below). This interpretation as such does not refute the notion of a possible reactivation of the shear zones during the Pyrenean orogeny, which was previously proposed by Mc Caig (1986) on the basis of Ar/Ar dating.

Variscan tectono-metamorphic evolution of the Central Pyrenees

Based on new structural and petrological observations, we propose hereafter a scenario for the Variscan tectono-metamorphic evolution of the Central Axial Zone of the Pyrenees.

During the first stage of Variscan evolution, the upper crust was affected by regional-scale folding, producing kilometre-scale open to tight southward verging folds with an east–west axial plane (Fig. 9a). We consider them as the first expression of Variscan transpression in the Axial Zone. At this time, the mid to lower crust (Infrastructure) was probably affected by upward-propagating HT–LP metamorphism (Fig. 9a). Note that faults recognized along the Pallaresa cross-section, with a subtractive character and apparent "north side down" movement (Port de Salau and Llavorsi faults), are folded and must have formed prior to this stage. Because of penetrative deformation that occurred during the next stage and of the difficulty to evaluate the amount of thickening, the thickness of each sedimentary unit in our reconstruction (Fig. 9a) remains speculative. Moreover, we consider the existence of a large syn-orogenic Carboniferous basin, similar to the Arreau bassin located a few kilometres to the west of the Palaressa cross-section (Delvolvé, 1987).

During the second stage of Variscan evolution, the upper crust was affected by intense horizontal shortening and vertical stretching producing multi-scale isoclinal folding and the formation of pervasive cleavage (Fig. 9b). In the central and northern part of the Axial Zone, the upper crust was affected by apparently coaxial shearing, while the southern part was the focus of non-coaxial "top-to-the-south" reverse kinematics, illustrating strain partitioning within the upper

crust. Non-coaxial shearing is responsible for the amplification of the overturned Pallaresa anticline (Fig. 9b). This event occurred at peak metamorphism, leading to the crystallization of biotite, muscovite and chlorite in cleavage planes.

During a third stage, strain localization occured with formation of 100-m-thick shear zones under amphibolite–greenschist conditions (Fig. 9c). The Lladorre and Estarón reverse shear zones were responsible for vertical offsets of the isotherms by ~ 2 km and 1 km, respectively. Similar displacement can be deduced from the offset of the sedimentary pile for the Lladorre shear zone (Fig. 4). At this stage, the dome shape of the Infrastructure was amplified by the displacement along shear zones (Fig. 9c). This interpretation is in agreement with structural observations made in the rest of the Axial Zone, where it has been shown that domes were lately amplified and affected by steep transpressional shear zones, showing retrogressive parageneses (Denèle, 2007; Vilà et al., 2007; Denèle et al., 2008, 2009).

Evolution of the Central Pyrenees during Cretaceous rifting and Pyrenean collision

Cretaceous rifting

The Cretaceous rifting event has strongly reworked the North Pyrenean Zone, which belongs to the European plate. Markers of this event correspond to: (i) late Aptian to early Cenomanian rift basins filled by flysch-type sediments (Debroas, 1987, 1990; Bodego et al., 2015; Chelalou et al., 2016); (ii) regional HT–LP metamorphism with temperatures locally reaching 600 °C (Vielzeuf & Kornprobst, 1984; Dauteuil & Ricou, 1989; Golberg & Leyreloup, 1990; Clerc & Lagabrielle, 2014; Vacherat et al., 2014) and widespread metasomatism (Schärer et al., 1999; Boulvais et al., 2007; Poujol et al., 2010; Fallourd et al., 2014; Boutin et al., 2016); (iii) exhumation of sub-continental mantle bodies (Fabries et al., 1991; Clerc et al., 2012; de Saint Blanquat et al., 2016).

By contrast, these markers of Cretaceous rifting are absent from the Axial Zone. Wherever present, the Mesozoic sediments unconformably deposited over the Variscan basement correspond to post-rift Cenomano-Turonian flysch (Ternet et al., 1980, 2003; Clin et al., 1986; Mirouse et al., 1993; Majeste-Menjoulas et al., 1999). In the Central Pyrenees, our structural and petrological study coupled with RSCM shows that (i) all vertical offsets display reverse motion, and (ii) the only thermal event recorded in the area is related to Variscan HT–LP metamorphism, with no sign of any later thermal overprint. These first-order observations suggest that the Axial Zone was relatively preserved during Cretaceous rifting. Evidence of Cretaceous rifting concern only the borders of the Axial Zone and remains scarce. Indeed, in the study area, Triassic ophites are described as intrusive into Paleozoic and Triassic sedimentary rocks in a fault zone near Couflens (Fig. 2; Ternet et al., 1997). Proximity between this fault zone and evidence of metasomatism with talc formation (Ternet et al., 1997) of Cretaceous age (Boutin et al., 2016) suggests fault (re)activation during the rifting event (Fig. 9d). In the western part of the Axial Zone, normal faulting is indicated by the remains of syn-rift deposits (Casteras et al., 1971; Ternet et al., 1980, 2003), which can be observed against the North-Pyrenean Fault. Along the North Pyrenean Fault east of the study area, evidence of major Cretaceous metasomatism has been discovered, with albitized rocks and talc occurrences (Fallourd et al., 2014). On the southern border of the Axial Zone, the formation of the Organyà Basin, which is described as a piggy-back basin with syn-rift Aptian to Albian deposits, is supposed to be related to a normal movement along the future Orri thrust (Fig. 9d, García Senz, 2002; Martinez-Peña & Casas-Sainz, 2003; Mencos et al., 2015).

Late Cretaceous to Cenozoic convergence

In the southern part of the Axial Zone, alpine movement along the Orri thrust is undeniable, highlighted by the Rialp window (Fig. 2 & 3), probably responsible for tilting of Variscan structures in the Orri anticline (Bons, 1988; Carreras & Debat, 1996). At depth, the Rialp thrust is

inferred from the ECORS seismic profile but has no geological incidence at the surface. Along the North Pyrenean Fault, Alpine deformation is marked by refolded Variscan structures and folds in Permo-Triassic sediments (Déramond, 1970; Ternet et al., 1997), as well as the reactivation of inherited vertical faults marked by the uplift of the northern blocks over several hundred metres to a few kilometres (Fig. 9d & e). Across the rest of the Axial Zone, there is no significant Alpine deformation, except in narrow corridors highlighted in Fig. 4 where crenulation cleavage was produced (Fig. 6b & 6c). So, except along the North Pyrenean Fault and few kilometres above the Orri thrust, no significant Alpine fault or penetrative deformation are observed, leading to the conclusion that Variscan structures appear continuous and mainly undisturbed in the central Axial Zone (Fig. 4).

Discussion

The constrasted response to Early Cretaceous rifting of the European and Iberian margins, which are represented respectively by the North-Pyrenean Zone and the Axial Zone, suggests an asymmetric rift system (Fig. 10a). The European margin of this rift shows a large distal domain, which comprises the inverted syn-rift basins of Camarade, Saint-Girons and Aulus (e.g. Mouthereau et al., 2014). The quantity of extension increased southward in this distal domain and has led to the exhumation close to the surface of mantle rocks in the Aulus Basin (Fig. 10a). These observations show that this rift system was mature and led to the breakup of the continental crust. By contrast, the Iberian margin shows a large proximal domain with the relatively preserved Axial Zone block and a restricted distal domain, localized near the North-Pyrenean fault zone. Asymmetrical conjugate margins have been evidenced in numerous purely extensional palaeo-rift systems (Chian et al., 1995; Ranero & Pérez-Gussinyé, 2010; Blaich et al., 2011; Espurt et al., 2012; Peron-Pinvidic et al., 2013; Sutra et al., 2013). However, a sinistral displacement has been deduced from motion of the Iberian plate in Cretaceous times (Le Pichon et al., 1970; Choukroune

et al., 1973; Choukroune & Mattauer, 1978; Olivet, 1996), suggesting that the Pyrenean rift system occurred under a transtensional stress regime. Furthermore, most of the syn-rift basins in the North-Pyrenean Zone of the Central Pyrenees correspond to narrow pull-apart basins (Debroas, 1987). In transtensional settings, strain can be partitioned into purely extensional domains and narrow strike-slip or transform faults (Allen et al., 1998; Wu et al., 2009), which could explain the degree of asymmetry of the Pyrenean rift system. Here we advocate that the North-Pyrenean Fault represents a transform fault that has accommodated the abrupt variation of extensional patterns between the Iberian and European plates during Cretaceous rifting (Fig. 10a). Further west, in the Basque massifs, the conjugate margins appear to be more symmetrical (Roca et al., 2011; Masini et al., 2014; Tugend et al., 2014) and the the North-Pyrenean Fault has never been identified. This feature highlights the segmentation of the Pyrenean rift system along the strike of the mountain belt.

Concerning the inversion of the rift system, classical models of the Pyrenean orogenic wedge have involved various basement thrust units in the Axial Zone and imply large-scale block rotations and internal deformation of these units (e.g. Beaumont et al., 2000). These basement units have been clearly identified in the western part of the Axial Zone, such as the Lakhora and Gavarnie units (Teixell, 1996), in its southernmost part with the Orri and Rialp units in the Central Pyrenees (e.g. Muñoz, 1992), and in the western Pyrenees with the Bielsa/Millares units (Teixell, 1996; Jolivet et al., 2007). Based on the interpretation of the ECORS seismic profile, Muñoz (1992) had proposed that the Nogueres sheet was rooted in the Axial Zone in the Central Pyrenees, and was an eastward prolongation of the Gavarnie thrust. In this currently accepted model, the Nogueres sheet would have been displaced to the south over a distance of 15–20 km (Berastegui et al., 1993; Beaumont et al., 2000). However, our results in the Axial Zone do not support such a model. We show instead that the main localized structures of the Central Pyrenees are ductile amphibolite to greenschist facies Variscan shear zones with only limited evidence of late

reactivation, and are associated with a motions that do not exceed 1–2 km (Figs. 4 & 7). Even if the reactivation of these Variscan shear zones was responsible for these kilometre-scale offsets, the evidence does not support the existence of a basement nappe rooted in the central part of the Axial Zone. Furthermore, despite intense deformation of the Superstructure during the Variscan orogeny, where upright isoclinal folds are common, the envelope of the stratigraphic markers remained roughly horizontal, as was that of the Infrastructure's roof and its metamorphic isograds (Figs. 4 & 7). Furthermore, thermochronogical data in Central Pyrenees show that the Nogueres unit and the Orri unit (Vergés et al., 1995, Teixell et al., 1998) have shared similar exhumation histories since late-Eocene times (Fig. 10c) (Fitzgerald et al., 1999; Sinclair et al., 2005). Consequently, the Central Pyrenees form a single tectonic unit, delimited by the North-Pyrenean Fault in the north and the Orri thrust in the south (Fig. 10b, Laumonier, 2015). In this scheme, the "têtes plongeantes" or "Plunging noses" (Séguret, 1972; Choukroune and Séguret, 1973) defined to the south of the Axial Zone should be reinterpreted as cover nappes originating in the Axial Zone or in the North Pyrenean Zone, and transported to its southern border by successive thrusting and décollements at the base of the Mesozoic cover and downward in the Silurian black shales. Given that the Nogueres allochtonous unit corresponds to the uppermost Paleozoic series and are devoid of syn-rift sequences as well as HT–MP metamorphic rocks that characterized the North Pyrenean massifs, we interpret this unit as belonging to the top of the Axial Zone. These cover nappes, which share the same exhumation histories as the Maladeta and Marimanha massifs (Fig. 10c), were disconnected from the Axial Zone by the exhumation of the Orri units in Oligocene times. If the amount of convergence of the Iberian plate, around 150 km since 83 Ma (Olivet, 1996; Sibuet et al., 2004; Vissers & Meijer, 2012) is correct, the estimates and the spatial distribution of shortening in the Pyrenean belt, especially within the Axial Zone, should be re-examined. Indeed, the total amount of convergence has been explained by a combination of subduction and crustal thickening (Beaumont et al., 2000). This later included 15–20 km of displacement of the Nogueres

nappe when considered as rooted in the Axial Zone. Furthermore, 10–15 km of shortening by pervasive internal deformation has been inferred in order to match the total convergence (Roure et al., 1989; Muñoz, 1992; Mouthereau et al., 2014). Given our interpretation of structures in the Central Pyrenees, these ca. 30 km of horizontal shortening by crustal thickening in the basement must be found elsewhere, for example in a greater amount of subduction of the Iberian plate.

The relative stability of the Axial Zone block since Paleozoic times highlighted the critical role of crustal-scale inherited structures from the Cretaceous rifting event on the geometry of the Cenozoic orogenic wedge. Convergence was first accommodated between 85 and 70 Ma within the thinned European margin, leading to the inversion of syn-rift basins and the accretion of microcontinental blocks that form the North Pyrenean massifs (Mouthereau et al., 2014; Ford et al., 2016; Vacherat et al., 2016) (Fig. 10b). Deformation then propagated southward during Eocene times into the moderately thinned Iberian crust, but remained focused around the main normal faults inherited from the Cretaceous. The reactivation of these normal faults as crustal-scale thrusts seems to have been sufficient to initiate the subduction of a part of the Iberian plate under the accreted European plate and the Axial Zone block, defining a pop-up structure (Fig. 10b; Brun, 2002). Given that the main shear zones of the Axial Zone remained preserved after Alpine collision, the role of inherited structures from the pre-rift events appears to be negligible in this scenario. The importance of the North-Pyrenean Fault, however, which formed a boundary between two continental margins with contrasting behaviours during rifting, and later between two contrasting pro- and retro-wedge domains during collision, is nonetheless also confirmed by our study. Most previous reconstructions had likewise considered that this fault was inherited from the Variscan orogenic cycle (Arthaud & Matte 1975; Burg, 1994; Carreras & Capella, 1994; Matte, 2001, Stampfli et al., 2013).

Conclusion

Our results provide a complete structural view of the architecture of the Axial Zone and its relationship with regional metamorphism in the Central Pyrenees. The present-day structure of the Central Pyrenees results from a multi-stage Variscan–Cretaceous–Alpine history. The central part of the Axial Zone represents an upper crustal sequence deformed under a transpressional regime in Variscan times, and is characterized by (i) regional to small-scale folds, (ii) steep penetrative axial-plane cleavage, and (iii) greenschist to amphibolite facies metamorphism associated to a HT–LP gradient. The flat pattern of Paleozoic stratigraphic and Variscan metamorphic markers all along the north–south cross-section of the Central Pyrenees, along with the absence of Cretaceous and Pyrenean crustal-scale faults in the core of the Axial Zone, highlight that this domain has been preserved from both rift- and collision-related overprints. Thus, in Cretaceous times, the Axial Zone formed a single continental bloc separated by the North Pyrenean Fault from the hyper-extended domain that formed the northern margin. Finally, the "Têtes plongeantes" units located south of the Axial Zone are re-interpreted here as cover nappes, detached from the central-southern upper part of the Axial Zone by faulting between the basement and the Mesozoic cover during the Cenozoic. In our model, the Axial Zone would thus correspond to a pop-up structure overthrusting its southern foreland. It contradicts the widely accepted view of an antiformal nappe stack in the core of the Axial Zone, previously elaborated by Muñoz (1992). Alpine shortening was restricted to the northern and southern borders of the Axial Zone, and focused around structures inherited from Cretaceous rifting.

Acknowledgements

This work was supported by the BRGM through the Référentiel Géologique de la France program (RGF). We thank D. Chardon, L. Jolivet, F. Mouthereau, J.-P. Brun, M. Ford, T. Poitrenaud and R. Augier for their fruitful discussion, as well as A. McCaig, B. Laumonier and

the subject editor Y. Gunnell for their constructive reviews. The structural data acquired for the study will be available on the RGF website (rgf.brgm.fr).

References

ALLEN, M.B., MACDONALD, D.I.M., XUN, Z., VINCENT, S.J. & BROUET-MENZIES, C. 1998. Transtensional deformation in the evolution of the Bohai Basin, northern China. *Geological Society, London, Special Publication*, **135**, 215–229, doi: 10.1144/GSL.SP.1998.135.01.14.

ANTOLÍN-TOMÁS, B., ROMÁN-BERDIEL, T., CASAS-SAINZ, A., GIL-PEÑA, I., OLIVA, B. & SOTO, R. 2009. Structural and magnetic fabric study of the Marimanha granite (Axial Zone of the Pyrenees). *International Journal of Earth Sciences*, **98**, 427–441, doi: 10.1007/s00531-007-0248-1.

ARTHAUD, F. & MATTE, P. 1975. Les decrochements tardi-hercyniens du sud-ouest de l'europe. Geometrie et essai de reconstitution des conditions de la deformation. *Tectonophysics*, **25**, 139–171, doi: 10.1016/0040-1951(75)90014-1.

BEAUMONT, C., MUÑOZ, J.A., HAMILTON, J. & FULLSACK, P. 2000. Factors controlling the Alpine evolution of the central Pyrenees inferred from a comparison of observations and geodynamical models. *Journal of Geophysical Research: Solid Earth*, **105**, 8121–8145, doi: 10.1029/1999JB900390.

BELLAHSEN, N., MOUTHEREAU, F., BOUTOUX, A., BELLANGER, M., LACOMBE, O., JOLIVET, L. & ROLLAND, Y. 2014. Collision kinematics in the western external Alps. *Tectonics*, **33**, 2013TC003453, doi: 10.1002/2013TC003453.

574 BERASTEGUI, X., LOSANTOS, M., MUÑOZ, J.A. & PUIGDEFABREGAS, C. 1993. Tall geològic del
575 Pirineu central, 1:200,000. *Publ. Geol. Catalunya*, 62 pp.

576 BESSIÈRE, G. 1987. *Modèle d'évolution polyorogénique d'un massif hercynien: le Massif de*
577 *Mouthoumet (Pyrénées Audoises)*. PhD thesis, Univ. Toulouse, France.

578 BEYSSAC, O., GOFFÉ, B., CHOPIN, C. & ROUZAUD, J.N. 2002. Raman spectra of carbonaceous
579 material in metasediments: a new geothermometer. *Journal of Metamorphic Geology*, **20**,
580 859–871, doi: 10.1046/j.1525-1314.2002.00408.x.

581 BICHOT, F. 1986. *La tectonique distensive carbonifère dans les Pyrénées. Corrélations est-*
582 *canadiennes et ouest-européennes*. PhD thesis, Univ. Bordeaux, France.

583 BLAICH, O.A., FALEIDE, J.I. & TSIKALAS, F. 2011. Crustal breakup and continent-ocean transition
584 at South Atlantic conjugate margins. *Journal of Geophysical Research: Solid Earth*, **116**,
585 B01402, doi: 10.1029/2010JB007686.

586 BODEGO, A., IRIARTE, E., AGIRREZABALA, L.M., GARCÍA-MONDÉJAR, J. & LÓPEZ-HORGUE, M.A.
587 2015. Synextensional mid-Cretaceous stratigraphic architecture of the eastern Basque–
588 Cantabrian basin margin (western Pyrenees). *Cretaceous Research*, **55**, 229–261, doi:
589 10.1016/j.cretres.2015.01.006.

590 BODIN, J. & LEDRU, P. 1986. Nappes hercyniennes précoces à matériel dévonien hétéropique dans
591 les Pyrénées ariégeoises. *Comptes Rendus de l'Académie des Sciences, Paris*, **302**, **II**, 969–
592 974.

593 BONS, A.J. 1988. Intracrystalline deformation and slaty cleavage development in very low-grade
594 slates from the Central Pyrenees. *Geologica Ultraiectina*, **56**.

595 BOUCHEZ, J.L. & GLEIZES, G. 1995. Two-stage deformation of the Mont-Louis-Andorra granite
596 pluton (Variscan Pyrenees) inferred from magnetic susceptibility anisotropy. *Journal of*
597 *the Geological Society*, **152**, 669–679, doi: 10.1144/gsjgs.152.4.0669.

598 BOULVAIS, P., RUFFET, G., CORNICHET, J. & MERMET, M. 2007. Cretaceous albitization and
599 dequartzification of Hercynian peraluminous granite in the Salvezines Massif (French
600 Pyrénées). *Lithos*, **93**, 89–106, doi: 10.1016/j.lithos.2006.05.001.

601 BOUTIN, A. 2016. *Étude des conditions de formation du gisement de talc-chlorite de Trimouns*
602 *(Ariège, France)*. PhD thesis, Univ. Toulouse, France.

603 BOUTIN, A., BLANQUAT, M. DE S., POUJOL, M., BOULVAIS, P., PARSEVAL, P. DE, ROULEAU, C. &
604 ROBERT, J.-F. 2016. Succession of Permian and Mesozoic metasomatic events in the
605 eastern Pyrenees with emphasis on the Trimouns talc–chlorite deposit. *International*
606 *Journal of Earth Sciences*, **105**, 747–770, doi: 10.1007/s00531-015-1223-x.

607 BRUN, J.-P. 2002. Deformation of the continental lithosphere: Insights from brittle-ductile models.
608 *Geological Society, London, Special Publication*, **200**, 355–370, doi:
609 10.1144/GSL.SP.2001.200.01.20.

610 BURG, J.-P., VAN DEN DRIESSCHE, J., BRUN, J.-P., 1994. Syn- to post-thickening extension in the
611 Variscan Belt of Western Europe: Mode and structural consequences. *Géologie de la*
612 *France*, **3**, 33–51.

613 CAPELLA, I. & BOU, O. 1997. La estructura del domo de la Rabassa y del sector oriental del
614 sinclinal de Llavorsí (Pirineo Central). *Estudios Geológicos*, **53**, 121–133, doi:
615 10.3989/egeol.97533-4237.

CAPELLA, I. & CARRERAS, J. 1996. La zonación estructural del hercínico del Pirineo Central en el anticlinorio de la Pallaresa. *Estudios Geológicos*, **52**, 51–61, doi: 10.3989/egeol.96521-2253.

CARRERAS, J. & CAPELLA, I. 1994. Structures and Tectonics at Different Lithospheric Levels Tectonic levels in the Palaeozoic basement of the Pyrenees: a review and a new interpretation. *Journal of Structural Geology*, **16**, 1509–1524, doi: 10.1016/0191-8141(94)90029-9.

CARRERAS, J. & DEBAT, P. (eds) 1996. Tectonique Hercynienne. *In*: *Synthèse Géologique et Géophysique des Pyrénées*. BRGM-ITGE, 501–584.

CASAS, J.M., DOMINGO, F., POBLET, J. & SOLER, A. 1989. On the role of the Hercynian and Alpine thrusts in the Upper Palaeozoic rocks of the Central and Eastern Pyrenees. *Geodinamica Acta*, **3**, 135–147, doi: 10.1080/09853111.1989.11105181.

CASAS, J.M., FERNÁNDEZ, O. & DOMINGO, F. 2007. Carboniferous normal faults in the Eastern Pyrenees: evidences and age constrains of syn-orogenic Variscan extension. *Geodinamica Acta*, **20**, 385–392, doi: 10.3166/ga.20.385-392.

CASTERAS, M., GOTTIS, M., CLIN, M., GUIGNARD, J.D., PARIS, J.-P., GALHARAGUE, J. & FREY, M. 1971. *Carte Géologique de la France (1/50 000), Feuille de Tardets Sorholus (1971)*, BRGM. Orléans.

CHELALOU, R., NALPAS, T., ET AL. 2016. New sedimentological, structural and paleo-thermicity data in the Boucheville Basin (eastern North Pyrenean Zone, France). *Comptes Rendus Géoscience*, **348**, 312–321, doi: 10.1016/j.crte.2015.11.008.

637 CHIAN, D., LOUDEN, K.E. & REID, I. 1995. Crustal structure of the Labrador Sea conjugate margin
638 and implications for the formation of nonvolcanic continental margins. *Journal of*
639 *Geophysical Research: Solid Earth*, **100**, 24239–24253, doi: 10.1029/95JB02162.

640 CHOUKROUNE, P. 1976. *Structure et évolution tectonique de la zone nord-pyrénéenne: analyse de*
641 *la déformation dans une portion de chaîne à schistosité sub-verticale*. Mémoire de la
642 Société Géologique de France, **127**, 176 p.

643 CHOUKROUNE, P. 1989. The Ecors Pyrenean deep seismic profile reflection data and the overall
644 structure of an orogenic belt. *Tectonics*, **8**, 23–39, doi: 10.1029/TC008i001p00023.

645 CHOUKROUNE, P. 1992. Tectonic evolution of the Pyrenees. *Annual Review of Earth and Planetary*
646 *Sciences*, **20**, 143–158.

647 CHOUKROUNE, P. & MATTAUER, M. 1978. Tectonique des Plaques et Pyrénées : sur le
648 fonctionnement de la faille transformante nord-pyrénéenne ; comparaisons avec des
649 modèles actuels. *Bulletin de la Société Géologique de France*, **XX**, 689–700.

650 CHOUKROUNE, P. & SÉGURET, M. 1973. Tectonics of the Pyrenees: role of compression and
651 gravity. *In*: De Jong, K.A., Scholten, R. (eds). *Gravity and Tectonics*. Wiley, 141–156.

652 CHOUKROUNE, P., SÉGURET, M. & GALDEANO, A. 1973. Caractéristiques et évolution structurale
653 des Pyrénées : un modèle de relations entre zone orogénique et mouvement des plaques.
654 *Bulletin de la Société Géologique de France*, **7**, 600–611.

655 CHOUKROUNE, P., ROURE, F. & PINET, B. 1990. Main results of the ECORS Pyrenees profile.
656 *Tectonophysics*, **173**, 411–423.

CLARIANA, P. 2001. Significado de los pliegues N-S en el área del río Civis. Sector oriental del flanco sur del sinclinal de Llavorsí (Zona Axial, Pirineos Centrales). *Boletín geológico y minero*, **112**, 39–46.

CLARIANA, P. & GARCÍA-SANSEGUNDO, J. 2009. Variscan structure in the eastern part of the Pallaresa massif, Axial Zone of the Pyrenees (NW Andorra). Tectonic implications. *Bulletin de la Société géologique de France*, **180**, 501–511, doi: 10.2113/gssgfbull.180.6.501.

CLERC, C. 2012. *Evolution du domaine nord-pyrénéen au Crétacé : amincissement crustal extrême et thermicite élevée : un analogue pour les marges passives*. PhD thesis, Univ. Paris 6, France.

CLERC, C. & LAGABRIELLE, Y. 2014. Thermal control on the modes of crustal thinning leading to mantle exhumation: Insights from the Cretaceous Pyrenean hot paleomargins. *Tectonics*, **33**, 2013TC003471, doi: 10.1002/2013TC003471.

CLERC, C., LAGABRIELLE, Y., NEUMAIER, M., REYNAUD, J.-Y. & BLANQUAT, M. DE S. 2012. Exhumation of subcontinental mantle rocks: evidence from ultramafic-bearing clastic deposits nearby the Lherz peridotite body, French Pyrenees. *Bulletin de la Société Géologique de France*, **183**, 443–459, doi: 10.2113/gssgfbull.183.5.443.

CLIN, M., LELONG, F., ET AL. 1986. *Carte Géologique de la France (1/50 000), Feuille Bagnères-de-Luchon (1084)*, BRGM, Orléans.

CLOKE, I.R., MOSS, S.J. & CRAIG, J. 1997. The influence of basement reactivation on the extensional and inversional history of the Kutai Basin, East Kalimantan, SE Asia. *Journal of the Geological Society*, **154**, 157–161, doi: 10.1144/gsjgs.154.1.0157.

679 COLCHEN, M., TERNET, Y., DEBROAS, E.J., DOMMANGET, A., GLEIZES, G., GUÉRANGÉ, B. &
680 ROUX, L. 1995. *Carte Géologique de la France (1/50 000), Feuille Aulus-Les-Bains*
681 *(1086)*, BRGM, Orléans.

682 CROCHET, B., VILLATTE, J., ET AL. 1989. *Carte Géologique de la France (1/50 000), Feuille*
683 *Quillan (1077)*, BRGM, Orléans.

684 DAUTEUIL, O. & RICOU, L.-E. 1989. Hot-fluid circulation as an origin for the North Pyrenean
685 Cretaceous metamorphism. *Geodinamica Acta*, **3**, 237–249, doi:
686 10.1080/09853111.1989.11105190.

687 DE SAINT BLANQUAT, M., BAJOLET, F., ET AL. 2016. Cretaceous mantle exhumation in the central
688 Pyrenees: New constraints from the peridotites in eastern Ariège (North Pyrenean zone,
689 France). *Comptes Rendus Geoscience*, **348**, 268–278, doi: 10.1016/j.crte.2015.12.003.

690 DE SITTER, L.U. & ZWART, H.J. 1962. Geological map of the Central Pyrenees. *Leidse Geologische*
691 *Mededelingen*, **27**, 191–369.

692 DEBROAS, E.J. 1987. Modele de bassin triangulaire a l'intersection de decrochements divergents
693 pour le fosse albo-cenomanien de la Ballongue (zone nord-pyreneenne, France). *Bulletin*
694 *de la Société Géologique de France*, **III**, 887–898, doi: 10.2113/gssgfbull.III.5.887.

695 DEBROAS, E.J. 1990. Le flysch noir albo-cénomanien témoin de la structuration albienne a
696 sénonienne de la Zone nord-pyrénéenne en Bigorre (Hautes-Pyrenees, France). *Bulletin de*
697 *la Société Géologique de France*, **VI**, 273–285, doi: 10.2113/gssgfbull.VI.2.273.

698 DELCHINI, S., LAHFID, A., PLUNDER, A. & MICHARD, A. 2016. Applicability of the RSCM
699 geothermometry approach in a complex tectono-metamorphic context: The Jebilet massif

case study (Variscan Belt, Morocco). *Lithos*, **256**–**257**, 1–12, doi: 10.1016/j.lithos.2016.04.007.

DELVOLVÉ, J.-J. 1987. *Un Bassin Synorogenique Varisque : Le Culm Des Pyrenees Centro-Occidentales*. PhD thesis, Univ. Toulouse 3, France.

DENÈLE, Y. 2007. *Formation Des Dômes Gneissiques Hercyniens Dans Les Pyrénées : Exemple Du Massif de l'Aston-Hospitalet*. PhD thesis, Univ. Toulouse 3, France.

DENÈLE, Y., OLIVIER, P. & GLEIZES, G. 2008. Progressive deformation of a zone of magma transfer in a transpressional regime: The Variscan Mérens shear zone (Pyrenees, France). *Journal of Structural Geology*, **30**, 1138–1149, doi: 10.1016/j.jsg.2008.05.006.

DENÈLE, Y., OLIVIER, P., GLEIZES, G. & BARBEY, P. 2009. Decoupling between the middle and upper crust during transpression-related lateral flow: Variscan evolution of the Aston gneiss dome (Pyrenees, France). *Tectonophysics*, **477**, 244–261, doi: 10.1016/j.tecto.2009.04.033.

DENÈLE, Y., LAUMONIER, B., PAQUETTE, J.-L., OLIVIER, P., GLEIZES, G. & BARBEY, P. 2014. Timing of granite emplacement, crustal flow and gneiss dome formation in the Variscan segment of the Pyrenees. *Geological Society, London, Special Publications*, **405**, 265–287, doi: 10.1144/SP405.5.

DÉRAMOND, J. 1970. *Tectoniques superposées dans le Paléozoïque du Haut-Salat (Pyrénées Ariégeoises)*. PhD thesis ("Thèse de 3e cycle"), Univ. Toulouse, France.

DÉRAMOND, J. 1979. *Déformation et Déplacement Des Nappes: Exemple de La Nappe de Gavarnie (Pyrénées Centrales)*. PhD thesis ("Thèse d'état"), Univ. Toulouse, France.

721 DUBOIS, P. & SEGUIN, J.C. 1978. Les flyschs Crétacé et Eocène de la zone commingeoise et leur
722 environnement. *Bulletin de la Société Géologique de France*, **S7**–**XX**, 657–671, doi:
723 10.2113/gssgfbull.S7-XX.5.657.

724 ESPURT, N., CALLOT, J.-P., ROURE, F., TOTTERDELL, J.M., STRUCKMEYER, H.I.M. & VIALLY, R.
725 2012. Transition from symmetry to asymmetry during continental rifting: an example from
726 the Bight Basin–Terre Adélie (Australian and Antarctic conjugate margins). *Terra Nova*,
727 **24**, 167–180, doi: 10.1111/j.1365-3121.2011.01055.x.

728 EVANS, N.G. 1993. *Deformation during the Emplacement of the Maladeta Granodiorite, Spanish*
729 *Pyrenees*. PhD thesis, Univ. Leeds.

730 EVANS, N.G., GLEIZES, G., LEBLANC, D. & BOUCHEZ, J.-L. 1997. Hercynian tectonics in the
731 Pyrenees: a new view based on structural observations around the Bassie`s granite pluton.
732 *Journal of Structural Geology*, **19**, 195–208, doi: 10.1016/S0191-8141(96)00080-6.

733 FABRIES, J., LORAND, J.-P., BODINIER, J.-L. & DUPUY, C. 1991. Evolution of the Upper Mantle
734 beneath the Pyrenees: Evidence from Orogenic Spinel Lherzolite Massifs. *Journal of*
735 *Petrology*, Special Volume, 55–76, doi: 10.1093/petrology/Special_Volume.2.55.

736 FALLOURD, S., POUJOL, M., BOULVAIS, P., PAQUETTE, J.-L., BLANQUAT, M. DE S. & RÉMY, P.
737 2014. In situ LA-ICP-MS U–Pb titanite dating of Na–Ca metasomatism in orogenic belts:
738 the North Pyrenean example. *International Journal of Earth Sciences*, **103**, 667–682, doi:
739 10.1007/s00531-013-0978-1.

740 FITZGERALD, P.G., MUÑOZ, J.A., CONEY, P.J. & BALDWIN, S.L. 1999. Asymmetric exhumation
741 across the Pyrenean orogen: implications for the tectonic evolution of a collisional orogen.
742 *Earth and Planetary Science Letters*, **173**, 157–170, doi: 10.1016/S0012-821X(99)00225-
743 3.

744 FORD, M., HEMMER, L., VACHERAT, A., GALLAGHER, K. & CHRISTOPHOUL, F. 2016. Retro-wedge
745 foreland basin evolution along the ECORS line, eastern Pyrenees, France. *Journal of the*
746 *Geological Society*, **173**, 419–437, doi: 10.1144/jgs2015-129.

747 GARCÍA SENZ, J. 2002. Cuencas extensivas del Cretácico Inferior en los Pirineos centrales.
748 Formación y subsecuente inversión. PhD thesis, Univ. Barcelona, Spain.

749 GARCIA-SANSEGUNDO, J. 1992. Estratigrafía y estructura de la Zona Axial pirenaica en la
750 transversal del Valle de Arán y de la Alta Ribagorça. *Publicaciones especiales del Boletín*
751 *Geológico y Minero*, ITGE, **103**, 1–290.

752 GARCÍA-SANSEGUNDO, J., POBLET, J., ALONSO, J.L. & CLARIANA, P. 2011. Hinterland-foreland
753 zonation of the Variscan orogen in the Central Pyrenees: comparison with the northern part
754 of the Iberian Variscan Massif. *Geological Society, London, Special Publications*, **349**,
755 169–184, doi: 10.1144/SP349.9.

756 GLEIZES, G. 1992. *Structure Des Granites Hercyniens Des Pyrénées de Mont-Louis-Andorre À La*
757 *Maladeta*. PhD thesis, Univ. Paul Sabatier,Toulouse, France.

758 GLEIZES, G., LEBLANC, D., SANTANA, V., OLIVIER, P. & BOUCHEZ, J.L. 1998. Sigmoidal structures
759 featuring dextral shear during emplacement of the Hercynian granite complex of
760 Cauterets–Panticosa (Pyrenees). *Journal of Structural Geology*, **20**, 1229–1245, doi:
761 10.1016/S0191-8141(98)00060-1.

762 GLEIZES, G., LEBLANC, D. & BOUCHEZ, J.L. 1998. The main phase of the Hercynian orogeny in
763 the Pyrenees is a dextral transpression. *Geological Society, London, Special Publications*,
764 **135**, 267–273, doi: 10.1144/GSL.SP.1998.135.01.17.

765 GOLBERG, J.M. & LEYRELOUP, A.F. 1990. High temperature-low pressure Cretaceous
766 metamorphism related to crustal thinning (Eastern North Pyrenean Zone, France).
767 *Contributions to Mineralogy and Petrology*, **104**, 194–207, doi: 10.1007/BF00306443.

768 GRETTER, N., RONCHI, A., LÓPEZ-GÓMEZ, J., ARCHE, A., DE LA HORRA, R., BARRENECHEA, J. &
769 LAGO, M. 2015. The Late Palaeozoic-Early Mesozoic from the Catalan Pyrenees (Spain):
770 60 Myr of environmental evolution in the frame of the western peri-Tethyan
771 palaeogeography. *Earth-Science Reviews*, **150**, 679–708, doi:
772 10.1016/j.earscirev.2015.09.001.

773 HARRISON, T. M., DUNCAN, I. & MCDOUGALL, I. 1985. Diffusion of ^{40}Ar in biotite: Temperature,
774 pressure an compositional effects. *Geochimica et Cosmochimica Acta*, **49**, 2461-2468, doi:
775 10.1016/0016-7037(85)90246-7.

776 HARTEVELT, J.J.A. 1970. Geology of the Upper Segre and Valira valleys, Central Pyrenees,
777 Andorra/Spain. *Leidse Geologische Mededelingen*, **45**, 161–236.

778 HIRTH, G. & TULLIS, J. 1992. Dislocation creep regimes in quartz aggregates. *Journal of Structural*
779 *Geology*, **14**, 145–159, doi: 10.1016/0191-8141(92)90053-Y.

780 IZQUIERDO-LLAVALL, E., CASAS-SAINZ, A.M. & OLIVA-URCIA, B. 2013. Heterogeneous
781 deformation recorded by magnetic fabrics in the Pyrenean Axial Zone. *Journal of*
782 *Structural Geology*, **57**, 97–113, doi: 10.1016/j.jsg.2013.10.005.

783 JOLIVET, M., LABAUME, P., MONIÉ, P., BRUNEL, M., ARNAUD, N. & CAMPANI, M. 2007.
784 Thermochronology constraints for the propagation sequence of the south Pyrenean
785 basement thrust system (France-Spain). *Tectonics*, **26**, TC5007, doi:
786 10.1029/2006TC002080.

787 KRETZ, R. 1983. Symbols for rock-forming minerals. *American Mineralogist*, **68**, 277–279.

788 LAGABRIELLE, Y. & BODINIER, J.-L. 2008. Submarine reworking of exhumed subcontinental
789 mantle rocks: field evidence from the Lherz peridotites, French Pyrenees. *Terra Nova*, **20**,
790 11–21, doi: 10.1111/j.1365-3121.2007.00781.x.

791 LAGABRIELLE, Y., LABAUME, P. & DE SAINT BLANQUAT, M. 2010. Mantle exhumation, crustal
792 denudation, and gravity tectonics during Cretaceous rifting in the Pyrenean realm (SW
793 Europe): Insights from the geological setting of the lherzolite bodies. *Tectonics*, **29**,
794 TC4012, doi: 10.1029/2009TC002588.

795 LAHFID, A., BEYSSAC, O., DEVILLE, E., NEGRO, F., CHOPIN, C. & GOFFÉ, B. 2010. Evolution of
796 the Raman spectrum of carbonaceous material in low-grade metasediments of the Glarus
797 Alps (Switzerland). *Terra Nova*, **22**, 354–360, doi: 10.1111/j.1365-3121.2010.00956.x.

798 LAUMONIER, B. 2015. Les Pyrénées alpines sud-orientales (France, Espagne) – essai de synthèse.
799 *Revue de Géologie Pyrénéenne*, **2**, 44 p. http://geologie-des-pyrenees.com/

800 LAUMONIER, B. (ED.). ET AL. 1996. Cambro-Ordovicien. *In*: *Barnolas A., Chiron J.C.: 'Synthèse*
801 *Géologique et Géophysique Des Pyrénées'*. BRGM-ITGE, 157–209.

802 LE PICHON, X., BONNIN, J. & SIBUET, J.-C. 1970. La faille nord-pyrénéenne : faille transformante
803 liée à l'ouverture du golfe de gascogne. *Comptes Rendus Académie des Sciences de Paris*,
804 **271**, 1941–1944.

805 LOSANTOS, M., PALAU, J. & SANZ, J. 1986. Considerations about Hercynian thrusting in the
806 Marimanya massif (central Pyrenees). *Tectonophysics*, **129**, 71–79, doi: 10.1016/0040-
807 1951(86)90246-5.

LUCAS, C. 1985. *Le grès rouge du versant nord des Pyrénées : essai sur la géodynamique de dépôts continentaux du Permien et du Trias*. PhD, Univ. Paul Sabatier, Toulouse, France.

MAJESTÉ-MENJOULAS, C. 1979. *Evolution alpine d'un segment de chaîne varisque: Nappe de Gavarnie, chevauchement Cinq-Monts-Gentiane (Pyrénées centrales et occidentales).* PhD, Univ. Paul Sabatier, Toulouse, France.

MAJESTÉ-MENJOULAS, C., DEBON, F., DRIOUCH, Y., FLACHERE, H., MOREAU, H., VALERO, J. & TERNET, Y. 1999. *Carte Géologique de la France (1/50 000), Feuille Gavarnie (1082).* BRGM, Orléans.

MARTINEZ-PEÑA, M. & CASAS-SAINZ, A. 2003. Cretaceous–Tertiary tectonic inversion of the Cotiella Basin (southern Pyrenees, Spain). *International Journal of Earth Sciences*, **92**, 99–113, doi: 10.1007/s00531-002-0283-x.

MASINI, E., MANATSCHAL, G., MOHN, G., GHIENNE, J.-F. & LAFONT, F. 2011. The tectono-sedimentary evolution of a supra-detachment rift basin at a deep-water magma-poor rifted margin: the example of the Samedan Basin preserved in the Err nappe in SE Switzerland. *Basin Research*, **23**, 652–677, doi: 10.1111/j.1365-2117.2011.00509.x.

MASINI, E., MANATSCHAL, G., TUGEND, J., MOHN, G. & FLAMENT, J.-M. 2014. The tectono-sedimentary evolution of a hyper-extended rift basin: the example of the Arzacq–Mauléon rift system (Western Pyrenees, SW France). *International Journal of Earth Sciences*, **103**, 1569–1596, doi: 10.1007/s00531-014-1023-8.

MATTE, P., 2001. The Variscan collage and orogeny (480-290Ma) and the tectonic definition of the Armorica microplate: a review. *Terra Nova*, **13**, 122–128, doi: 10.1046/j.1365-3121.2001.00327.x.

MAUREL, O., MONIÉ, P., PIK, R., ARNAUD, N., BRUNEL, M. & JOLIVET, M. 2008. The Meso-Cenozoic thermo-tectonic evolution of the Eastern Pyrenees: an $^{40}Ar/^{39}Ar$ fission track and (U-Th)/He thermochronological study of the Canigou and Mont-Louis massifs. *International Journal of Earth Sciences*, **97**, 565–584, doi: 10.1007/s00531-007-0179-x.

MCCAIG, A. 1986. Thick- and thin-skinned tectonics in the Pyrenees. *Tectonophysics*, **129**, 319–342, doi: 10.1016/0040-1951(86)90259-3.

MCCAIG, A. & MILLER, J.A. 1986. $^{40}Ar/^{39}Ar$ age of mylonites along the Mérens fault, Central Pyrenees. *Tectonophysics*, **129**, 149–172, doi: 10.1016/0040-1951(86)90250-7.

MCINTOSH, K., AVENDONK, H. VAN, ET AL. 2013. Inversion of a hyper-extended rifted margin in the southern Central Range of Taiwan. *Geology*, **41**, 871–874, doi: 10.1130/G34402.1.

MENCOS, J., CARRERA, N. & MUÑOZ, J.A. 2015. Influence of rift basin geometry on the subsequent postrift sedimentation and basin inversion: The Organyà Basin and the Bóixols thrust sheet (south central Pyrenees). *Tectonics*, **34**, 2014TC003692, doi: 10.1002/2014TC003692.

MESALLES, L., MOUTHEREAU, F., BERNET, M., CHANG, C.-P., LIN, A.T.-S., FILLON, C. & SENGELEN, X. 2014. From submarine continental accretion to arc-continent orogenic evolution: The thermal record in southern Taiwan. *Geology*, **42**, 907–910, doi: 10.1130/G35854.1.

METCALF, J.R., FITZGERALD, P.G., BALDWIN, S.L. & MUÑOZ, J.-A. 2009. Thermochronology of a convergent orogen: Constraints on the timing of thrust faulting and subsequent exhumation of the Maladeta Pluton in the Central Pyrenean Axial Zone. *Earth and Planetary Science Letters*, **287**, 488–503, doi: 10.1016/j.epsl.2009.08.036.

MEY, P.H.W. 1968. The geology of the upper Ribagorzana and Tor Valleys, Central Pyrenees, Spain sheet 8, 1: 50000. *Leidse Geologische Mededelingen*, **41**, 229–292.

MEZGER, J.E. 2005. Comparison of the western Aston-Hospitalet and the Bossòst domes: Evidence for polymetamorphism and its implications for the Variscan tectonic evolution of the Axial Zone of the Pyrenees. *Journal of the Virtual Explorer*, **19**, doi: 10.3809/jvirtex.2005.00122.

MEZGER, J.E. 2009. Transpressional tectonic setting during the main Variscan deformation: evidence from four structural levels in the Bossòst and Aston-Hospitalet mantled gneiss domes, central Axial Zone, Pyrenees. *Bulletin de la Société Géologique de France*, **180**, 199–207, doi: 10.2113/gssgfbull.180.3.199.

MEZGER, J.E. & PASSCHIER, C.W. 2003. Polymetamorphism and ductile deformation of staurolite–cordierite schist of the Bossòst dome: indication for Variscan extension in the Axial Zone of the central Pyrenees. *Geological Magazine*, **140**, 595–612, doi: 10.1017/S0016756803008112.

MEZGER, J.E. & REGNIER, J.-L. 2016. Stable staurolite–cordierite assemblages in K-poor metapelitic schists in Aston and Hospitalet gneiss domes of the central Pyrenees (France, Andorra). *Journal of Metamorphic Geology*, **34**, 167–190, doi: 10.1111/jmg.12177.

MIROUSE, R., BARRÈRE, P., ET AL. 1993. *Carte Géol. France (1/50 000), Feuille Vielle-Aure (1083)*. BRGM, Orléans.

MOHN, G., MANATSCHAL, G., BELTRANDO, M., MASINI, E. & KUSZNIR, N. 2012. Necking of continental crust in magma-poor rifted margins: Evidence from the fossil Alpine Tethys margins. *Tectonics*, **31**, TC1012, doi: 10.1029/2011TC002961.

MONIÉ, P., SOLIVA, J., BRUNEL, M. & MALUSKI, H. 1994. Les cisaillements mylonitiques du granite de Millas (Pyrénées, France). Age Crétacé $^{40}Ar/^{39}Ar$ et interprétation tectonique. *Bulletin de la Société Géologique de France*, **165**, 559–571.

MOUTHEREAU, F. & LACOMBE, O. 2006. Inversion of the Paleogene Chinese continental margin and thick-skinned deformation in the Western Foreland of Taiwan. *Journal of Structural Geology*, **28**, 1977–1993, doi: 10.1016/j.jsg.2006.08.007.

MOUTHEREAU, F., LACOMBE, O. & VERGÉS, J. 2012. Building the Zagros collisional orogen: Timing, strain distribution and the dynamics of Arabia/Eurasia plate convergence. *Tectonophysics*, **532**–**535**, 27–60, doi: 10.1016/j.tecto.2012.01.022.

MOUTHEREAU, F., WATTS, A.B. & BUROV, E. 2013. Structure of orogenic belts controlled by lithosphere age. *Nature Geoscience*, **6**, 785–789, doi: 10.1038/ngeo1902.

MOUTHEREAU, F., FILLEAUDEAU, P.-Y., ET AL. 2014. Placing limits to shortening evolution in the Pyrenees: Role of margin architecture and implications for the Iberia/Europe convergence. *Tectonics*, **33**, 2014TC003663, doi: 10.1002/2014TC003663.

MUÑOZ, J.A. 1992. Evolution of a continental collision belt: ECORS-Pyrenees crustal balanced cross-section. *In*: *Thrust Tectonics*, edited by K.R. McClay, 235–246, Chapman & Hall, London, doi: 10.1007/978-94-011-3066-0_21.

OLIVET, J.-L. 1996. La cinématique de la plaque ibérique. *Bulletin des Centres de Recherches Exploration Production Elf-Aquitaine*, **20**, 131–195.

PAQUETTE, J.-L., GLEIZES, G., LEBLANC, D. & BOUCHEZ, J.-L. 1997. Le granite de Bassiès (Pyrénées) : un pluton syntectonique d'âge Westphalien. Géochronologie U-Pb sur zircons. *Comptes Rendus de l'Académie des Sciences, Paris*, **324**, 387–392.

PERON-PINVIDIC, G., MANATSCHAL, G. & OSMUNDSEN, P.T. 2013. Structural comparison of archetypal Atlantic rifted margins: A review of observations and concepts. *Marine and Petroleum Geology*, **43**, 21–47, doi: 10.1016/j.marpetgeo.2013.02.002.

POUJOL, M., BOULVAIS, P. & KOSLER, J. 2010. Regional-scale Cretaceous albitization in the Pyrenees: evidence from in situ U–Th–Pb dating of monazite, titanite and zircon. *Journal of the Geological Society*, **167**, 751–767, doi: 10.1144/0016-76492009-144.

RANERO, C.R. & PÉREZ-GUSSINYÉ, M. 2010. Sequential faulting explains the asymmetry and extension discrepancy of conjugate margins. *Nature*, **468**, 294–299, doi: 10.1038/nature09520.

ROCA, E., MUÑOZ, J.A., FERRER, O. & ELLOUZ, N. 2011. The role of the Bay of Biscay Mesozoic extensional structure in the configuration of the Pyrenean orogen: Constraints from the MARCONI deep seismic reflection survey. *Tectonics*, **30**, TC2001, doi: 10.1029/2010TC002735.

ROEST, W.R. & SRIVASTAVA, S.P. 1991. Kinematics of the plate boundaries between Eurasia, Iberia, and Africa in the North Atlantic from the Late Cretaceous to the present. *Geology*, **19**, 613–616, doi: 10.1130/0091-7613(1991)019<0613:KOTPBB>2.3.CO;2.

ROURE, F., CHOUKROUNE, P., ET AL. 1989. ECORS deep seismic data and balanced cross sections: Geometric constraints on the evolution of the Pyrenees. *Tectonics*, **8**, 41–50.

SCHÄRER, DE PARSEVAL, POLVÉ & DE SAINT BLANQUAT. 1999. Formation of the Trimouns talc-chlorite deposit (Pyrenees) from persistent hydrothermal activity between 112 and 97 Ma. *Terra Nova*, **11**, 30–37, doi: 10.1046/j.1365-3121.1999.00224.x.

SÉGURET, M. 1972. *Etude tectonique des nappes et séries décollées de la partie centrale du versant sud des Pyrénées : caractère synsédimentaire, rôle de la compression et de la gravité*. PhD thesis, Univ. Montpellier, France.

SIBUET, J.-C., SRIVASTAVA, S.P. & SPAKMAN, W. 2004. Pyrenean orogeny and plate kinematics. *Journal of Geophysical Research: Solid Earth*, **109**, B08104, doi: 10.1029/2003JB002514.

SINCLAIR, H.D., GIBSON, M., NAYLOR, M. & MORRIS, R.G. 2005. Asymmetric growth of the Pyrenees revealed through measurement and modeling of orogenic fluxes. *American Journal of Science*, **305**, 369–406, doi: 10.2475/ajs.305.5.369.

SOLER, D., TEIXELL, A. & GARCÍA-SANSEGUNDO, J. 1998. Amortissement latéral du chevauchement de Gavarnie et sa relation avec les unités sud-pyrénéennes. *Comptes Rendus de l'Académie des Sciences, Paris*, **327**, 699–704, doi: 10.1016/S1251-8050(99)80028-7.

SONG, W.J. & REE, J.-H. 2007. Effect of mica on the grain size of dynamically recrystallized quartz in a quartz–muscovite mylonite. *Journal of Structural Geology*, **29**, 1872–1881, doi: 10.1016/j.jsg.2007.09.011.

SOULAIMANI, A. & BURKHARD, M. 2008. The Anti-Atlas chain (Morocco): the southern margin of the Variscan belt along the edge of the West African craton. *Geological Society, London, Special Publications*, **297**, 433–452, doi: 10.1144/SP297.20.

STAMPFLI, G.M., HOCHARD, C., VÉRARD, C., WILHEM, C., VONRAUMER, J. 2013. The formation of Pangea. *Tectonophysics*, **593**, 1–19, doi: 10.1016/j.tecto.2013.02.037.

STIPP, M., STÜNITZ, H., HEILBRONNER, R. & SCHMID, S.M. 2002. The eastern Tonale fault zone: a 'natural laboratory' for crystal plastic deformation of quartz over a temperature range

938 from 250 to 700 °C. *Journal of Structural Geology*, **24**, 1861–1884, doi: 10.1016/S0191-
939 8141(02)00035-4.

940 SUTRA, E., MANATSCHAL, G., MOHN, G. & UNTERNEHR, P. 2013. Quantification and restoration
941 of extensional deformation along the Western Iberia and Newfoundland rifted margins.
942 *Geochemistry, Geophysics, Geosystems*, **14**, 2575–2597, doi: 10.1002/ggge.20135.

943 TEIXELL, A. 1996. The Ansó transect of the southern Pyrenees: basement and cover thrust
944 geometries. *Journal of the Geological Society*, **153**, 301–310, doi:
945 10.1144/gsjgs.153.2.0301.

946 TERNET, Y., BARRÈRE, P., ET AL. 1980. *Carte Géologique de la France (1/50 000), Feuille*
947 *Argelès-Gazost (1070)*, BRGM. BRGM, Orléans.

948 TERNET, Y., COLCHEN, M., ET AL. 1997. *Notice Explicative, Carte Géol. France (1/50 000),*
949 *Feuille Aulus-Les-Bains (1086)*, BRGM, Orléans.

950 TERNET, Y., BARRÈRE, P., CANEROT, J. & MAJESTE-MENJOULAS, C. 2003. *Carte Géologique de*
951 *la France (1/50 000), Feuille Laruns-Somport (1069)*. BRGM, Orléans.

952 TRIBOULET, C., GUITARD, G., KATONA, I. & NAVIDAD, M. 2005. Évolution pression–température
953 des amphibolites de la zone axiale au cours du métamorphisme hercynien des Pyrénées
954 orientales. *Comptes Rendus Geoscience*, **337**, 1244–1249, doi: 10.1016/j.crte.2005.06.011.

955 TUGEND, J., MANATSCHAL, G., KUSZNIR, N.J., MASINI, E., MOHN, G. & THINON, I. 2014.
956 Formation and deformation of hyperextended rift systems: Insights from rift domain
957 mapping in the Bay of Biscay-Pyrenees. *Tectonics*, **33**, 2014TC003529, doi:
958 10.1002/2014TC003529.

VACHERAT, A., MOUTHEREAU, PIK, R., BERNET, M., GAUTHERON, C., MASINI, E., LE POURHIET, L., TIBARI, B., LAHFID, A. 2014. Thermal imprint of rift-related processes in orogens as recorded in the Pyrenees. *Earth and Planetary Science Letters*, **408**, 296–306, doi: 10.1016/j.epsl.2014.10.014.

VACHERAT, A., MOUTHEREAU, F., PIK, R., BELLAHSEN, N., GAUTHERON, C., BERNET, M., DAUDET, M., BALANSA, J., TIBARI, B., JAMME, R. P., RADAL, J. 2016. Rift-to-collision transition recorded by tectonothermal evolution of the northern Pyrenees. *Tectonics*, **35**, 2015TC004016, doi: 10.1002/2015TC004016.

VAUCHEZ, A., CLERC, C., BESTANI, L., LAGABRIELLE, Y., CHAUVET, A., LAHFID, A. & MAINPRICE, D. 2013. Preorogenic exhumation of the North Pyrenean Agly massif (Eastern Pyrenees-France). *Tectonics*, **32**, 95–106, doi: 10.1002/tect.20015.

VERGELY, P. 1970. *Étude tectonique des structures pyrénéennes du versant sud des Pyrénées Orientales entre le rio Lliobregat et le rio Ter, province de Barcelone et de Gerone, Espagne*. PhD thesis, Univ. Montpellier, France.

VERGÉS, J., MILLAN, H., ET AL. 1995. Eastern Pyrenees and related foreland basins: pre-, syn- and post-collisional crustal-scale cross-sections. *Marine and Petroleum Geology*, **12**, 903–915, doi: 10.1016/0264-8172(95)98854-X.

VERGÉS, J., FERNÀNDEZ, M. & MARTÍNEZ, A. 2002. The Pyrenean orogen: pre-, syn-, and post-collisional evolution. *Journal of the Virtual Explorer*, **8**, 55–74.

VIELZEUF, D. & KORNPROBST, J. 1984. Crustal splitting and the emplacement of Pyrenean lherzolites and granulites. *Earth and Planetary Science Letters*, **67**, 87–96, doi: 10.1016/0012-821X(84)90041-4.

VILÀ, M., PIN, C., LIESA, M. & ENRIQUE, P. 2007. LPHT metamorphism in a late orogenic transpressional setting, Albera Massif, NE Iberia: implications for the geodynamic evolution of the Variscan Pyrenees. *Journal of Metamorphic Geology*, **25**, 321–347, doi: 10.1111/j.1525-1314.2007.00698.x.

VISSERS, R.L.M. & MEIJER, P.T. 2012. Iberian plate kinematics and Alpine collision in the Pyrenees. *Earth-Science Reviews*, **114**, 61–83, doi: 10.1016/j.earscirev.2012.05.001.

VISSERS, R.L.M. VAN HINSBERGEN, D.J.J., WILKINSON, C.M. & GANERØD, M. 2017. Middle Jurassic shear zones at Cap de Creus (eastern Pyrenees, Spain): a record of pre-drift extension of the Piemonte–Ligurian Ocean? *Journal of the Geological Society*, **174**, 289–300, doi:10.1144/jgs2016-014

WAYNE, D. M. & MCCAIG, A. M. 1998. Dating fluid flow in shear zones: Rb-Sr and U-Pb studies of syntectonic veins in the Néouvielle Massif, Pyrenees. *Geological Society, London, Special Publications*, **144**, 129–135, doi: 10.1144/GSL.SP.1998.144.01.09.

WROBEL-DAVEAU, J.-C., RINGENBACH, J.-C., TAVAKOLI, S., RUIZ, G.M.H., MASSE, P. & LAMOTTE, D.F. DE. 2010. Evidence for mantle exhumation along the Arabian margin in the Zagros (Kermanshah area, Iran). *Arabian Journal of Geosciences*, **3**, 499–513, doi: 10.1007/s12517-010-0209-z.

WU, J.E., MCCLAY, K., WHITEHOUSE, P. & DOOLEY, T. 2009. 4D analogue modelling of transtensional pull-apart basins. *Marine and Petroleum Geology*, **26**, 1608–1623, doi: 10.1016/j.marpetgeo.2008.06.007.

ZANDVLIET, J. 1960. The geology of the upper Salat and Pallaresa valleys, Central Pyrenees, France/Spain. *Leidse Geologische Mededelingen*, **25**, 1–127.

ZWART, H.J. 1979. The geology of the Central Pyrenees. *Leidse Geologische Mededelingen*, **50**, 1–74.

ZWART, H.J. 1986. The Variscan geology of the Pyrenees. *Tectonophysics*, **129**, 9–27.

ZWART, H.J., ROBERTI, K.F., ET AL. 1976. *Geological Map of the Central Pyrenees. Sheet 9. Flamisell-Pallaresa (Spain). Scale 1/50,000*. Geological Institute, University of Leiden.

Figure captions:

Figure 1: (**a**) Location of the Variscan crust of the Pyrenees in western Europe, with main Mesozoic basins. 1- Organyà basin, 2- Arzacq-Mauléon basin, 3- Parentis basin, 4- Basco-Cantabrian and le Danois basins, 5- Central Iberian basins (Tugend et al., 2014); (**b**) Geological sketch map of the Variscan crust of the Pyrenees. In blue: main Alpine faults; in black: main Variscan shear zones. Abbreviations: ELT: Les Eaux Chaudes/Lakhora Thrust; GT: Gavarnie Thrust; NPF: North Pyrenean Fault, LT: Llavorsi thrust, MSZ: Mérens Shear Zone). (**c**) Tectonic subdivision of the Axial Zone (Mouthereau et al. 2014).

Figure 2: Geological map of the Central Pyrenees, modified from Colchen et al. (1995) and Zwart et al. (1976) showing location of the Pallaresa cross-section presented in this work (Fig. 4). Studied outcrop and samples for RSCM measurements are also reported.

Figure 3: (**a**) Structural map of the Central Pyrenees. In grey: Upper Paleozoic rocks; in white: Cambrian to Ordovician rocks; in orange and pink: Variscan domes and granitoids, respectively. In blue: stretching lineations and kinematics from Evans et al. (1997). Data compiled for cleavage trajectories are from Mey (1968), Hartevelt (1970), Colchen et al. (1995), Evans et al. (1997),

Mezger (2005) (Aston metamorphic dome), and from our observations (n=300). Foliation trajectories in plutons were deduced from AMS studies by Gleizes (1992), Evans et al. (1997) and Antolín-Tomás et al. (2009). (**b**) S1 (black) and Sa (blue) schistosity poles from our measurements. (**c**) L1 mineral-stretching lineations measured in the field in black, and Fa fold axes in blue. Stereograms: lower hemisphere, equal area projection. Contours at 2σ are calculated for black points (i.e. S1 and L1).

Figure 4: N–S geological cross-section of the Central Pyrenees. Only significant alpine corridors that have been observed or rigorously described in the litterature are represented on this cross-section.

Figure 5: Field photographs illustrating the mains structures described in the text. (**a**) Undeformed Lower to Middle Triassic sandstones and conglomerates; bedding is sub-horizontal and sedimentary figures attest normal polarity (Location: Port del Canto, Rubiò); Photograph (**b**) and interpretative sketch (**b**') of penetrative axial-plane cleavage in siltites and sandstones (Location: South of Alós d'Isil); (**c**) Asymmetrical boudinated sandstones in marbles of the Lladorre shear zone, showing north-side-up kinematics ; (**d**) C' shears with top-to-the-south kinematics in Upper Ordovician conglomerates (Location: Cardós valley).

Figure 6: (**a**) Asymetrical boudinated quartz veins within Cambro-Ordovician sandstones showing dextral kinematics (Location: south of the Port de Marterat, western part of the country-rocks of the Bassiès pluton); (**b**) Apparent obliquity between the regional schistosity S0-1 and the late crenulation cleavage associated to kink-bands (Same location than Fig. 6a & 6b); (**c**) Longitudinal late folds and associated crenulation cleavage Sa steeply dipping to the south and affecting the regional schistosity S0-1 (Location: 400m north of Ainet de Cardós).

Figure 7: (**a**) Palaeotemperatures obtained by Raman Spectroscopy of Carbonaceous Material (RSCM). Error bars are standard deviation. X-axis corresponds to the latitude; (**b**) Interpreted position of isotherms in our cross-section deduced from RSCM data and petrological descriptions.

Figure 8: Microphotographs of various rocks of the Pallaresa. Bt: biotite, Ms: muscovite, Chl: chlorite. Explanations are in the text. (**a**) Precambrian schist of the Palarressa anticline (sample 15BL106). (**b**) Microphotograph of a muscovite-bearing schist. Schistosity, underlined by muscovite, with dip around 30° to the north and inflected by a "top-to-the-south" C' shear band. (**c** and **d**) Quartz pebble of the Upper Ordovician conglomerate showing dynamic recrystallization: bugling in (**c**) and sub-grain rotation in (**d**). (**e**) Chlorite-bearing schist of the Orri anticline. Sa: Steep alpine cleavage, S1: main schistosity (S1).

Figure 9: Tectonic evolution of the Axial Zone. Further explanations are in the text.

Figure 10: (**a**) 3D bloc-diagram of the Cretaceous transcurrent rifting mode in the Pyrenees ; (**b**) 3D bloc-diagram showing the lithospheric architecture of the Central Pyrenean belt. Interpretation of deep structures from Choukroune (1989) and Muñoz (1992), except in the Axial Zone. Massifs with apatite fission-track data in the Central Pyrenees are represented. In brown, the Nogueres cover nappes; (**c**) Apatite fission-track ages obtained in the Central Axial Zone by Fitzgerald et al. (1999), Sinclair et al. (2005), and Metcalf et al. (2009), plotted together in an age–elevation plot.

Figure 1

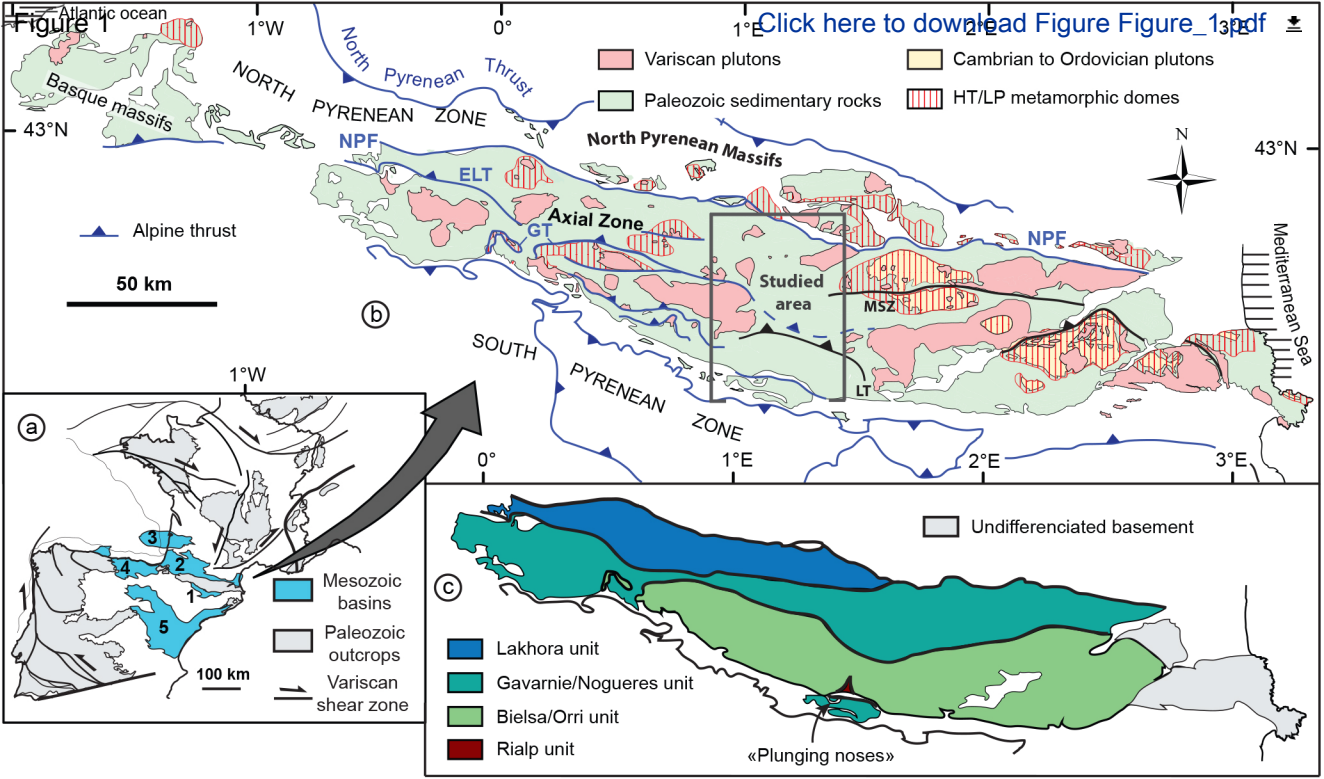

Cochelin et al., Figure 1

Figure 2

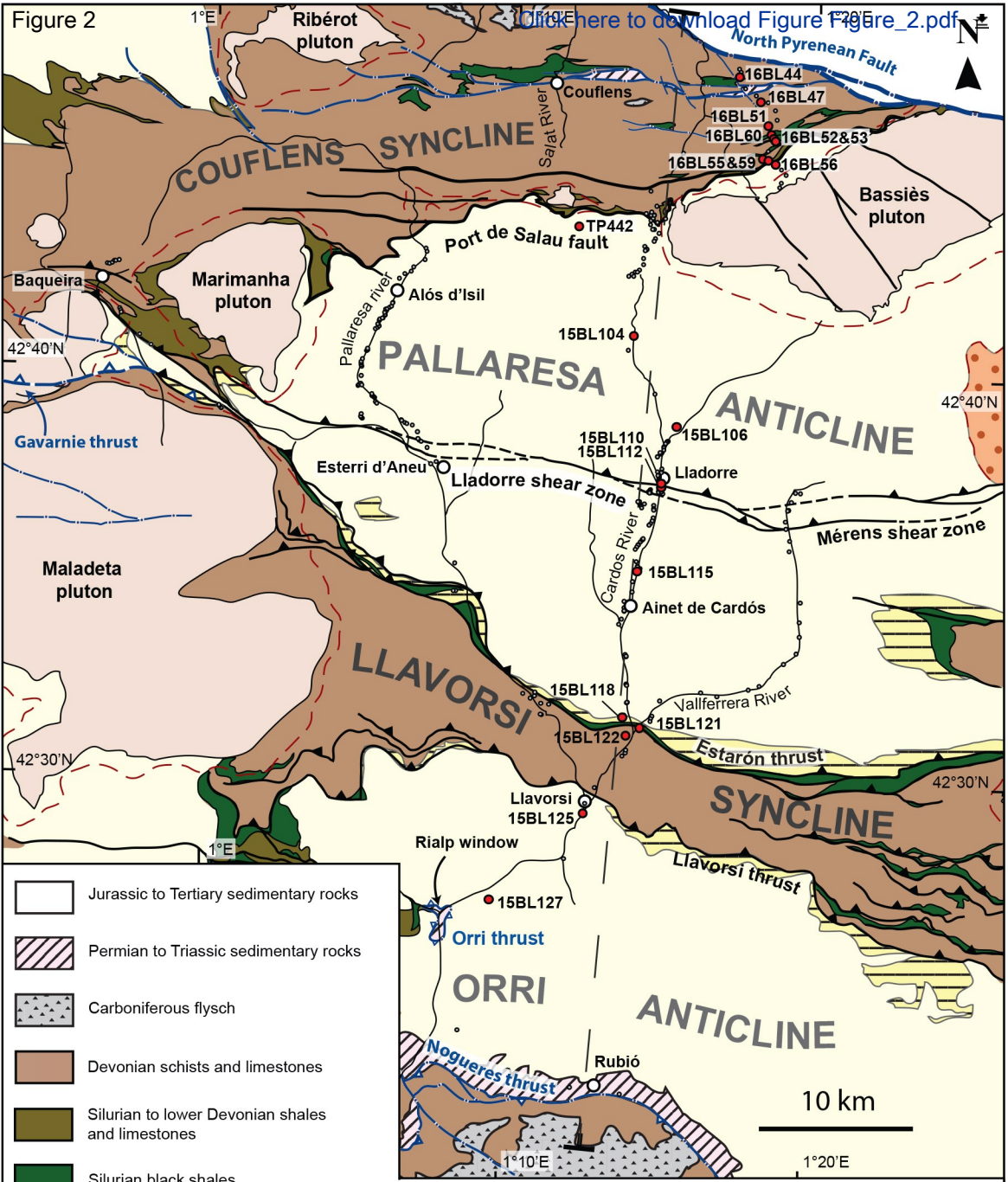

Cochelin et al., Figure 2

Figure 3

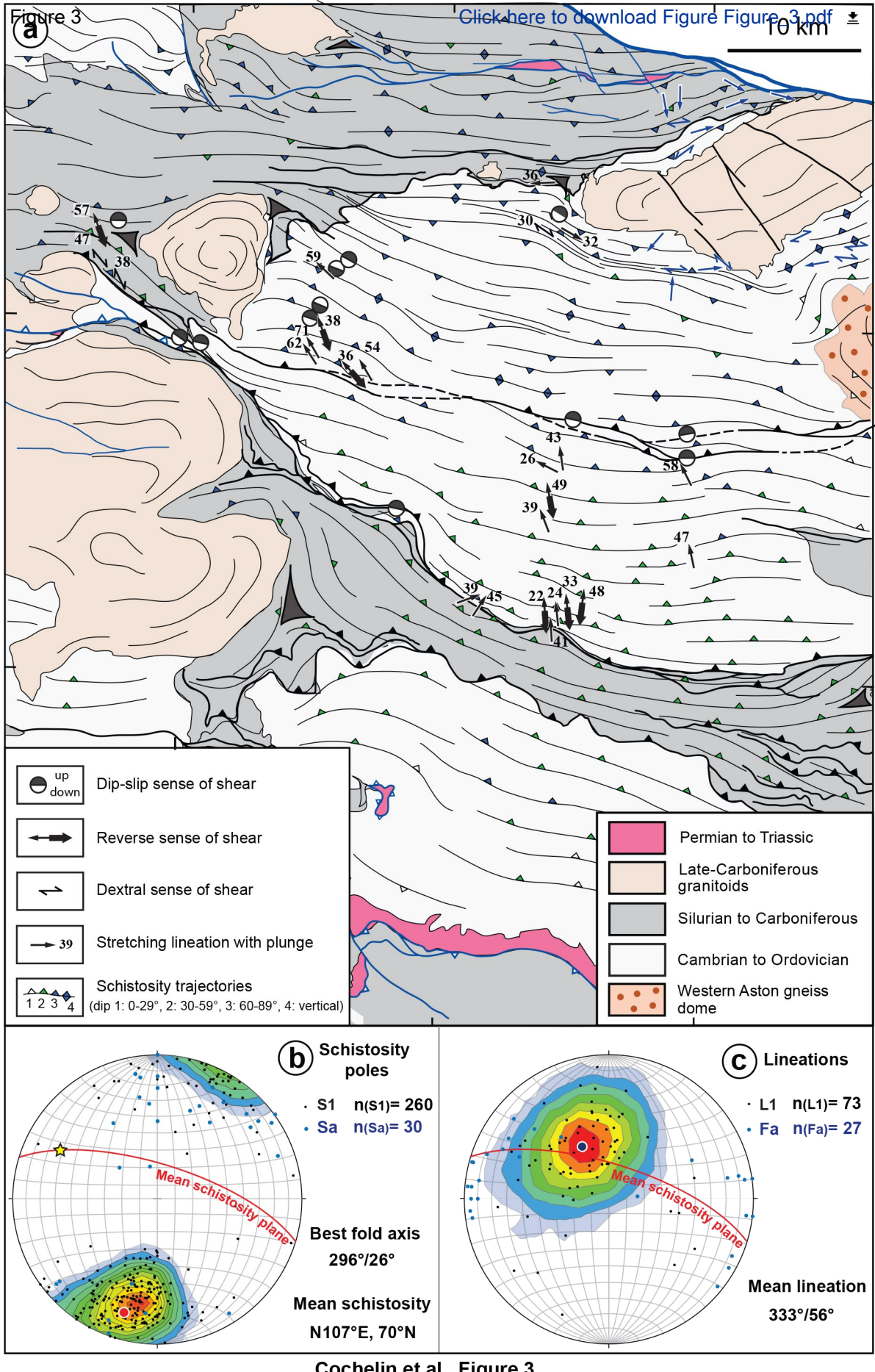

Cochelin et al., Figure 3

Figure 4

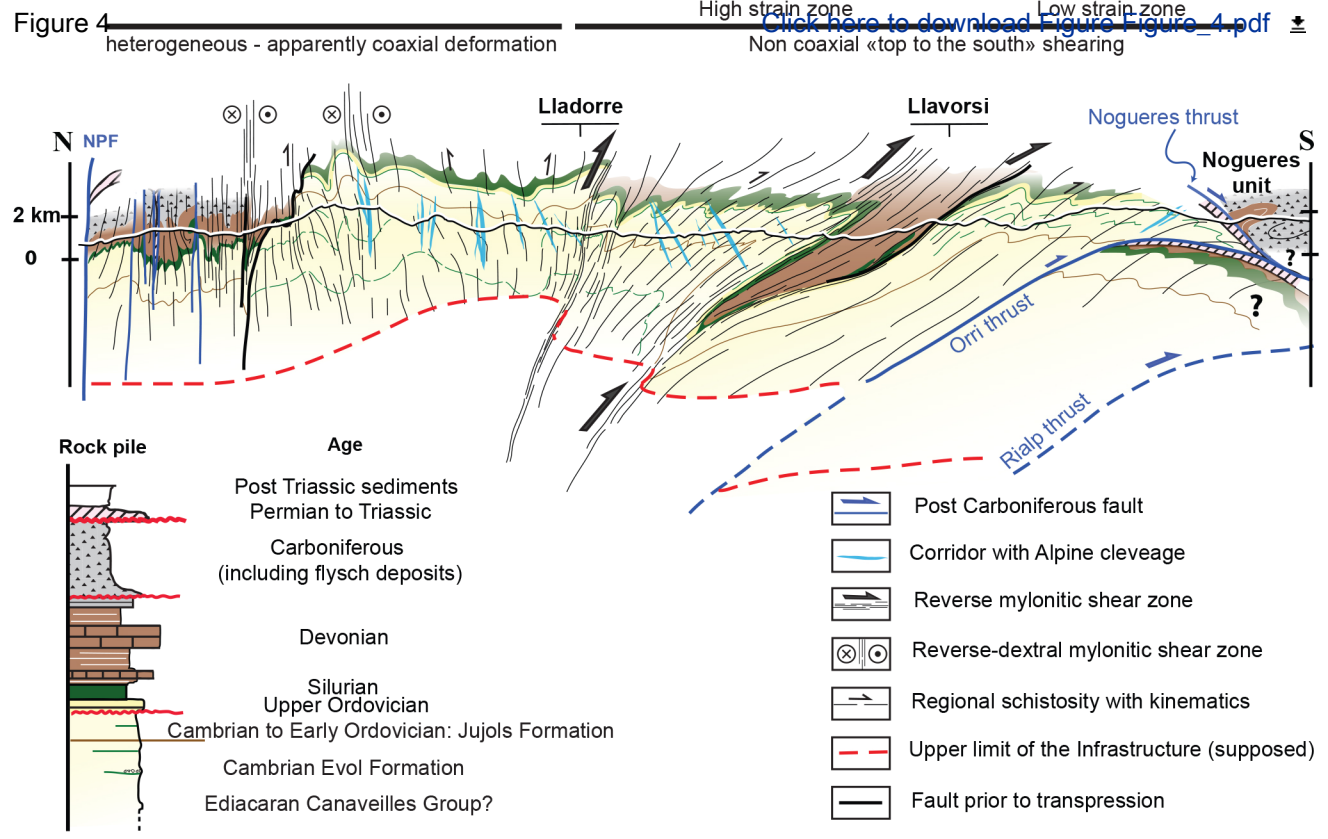

Cochelin et al. Figure 4

Figure 5

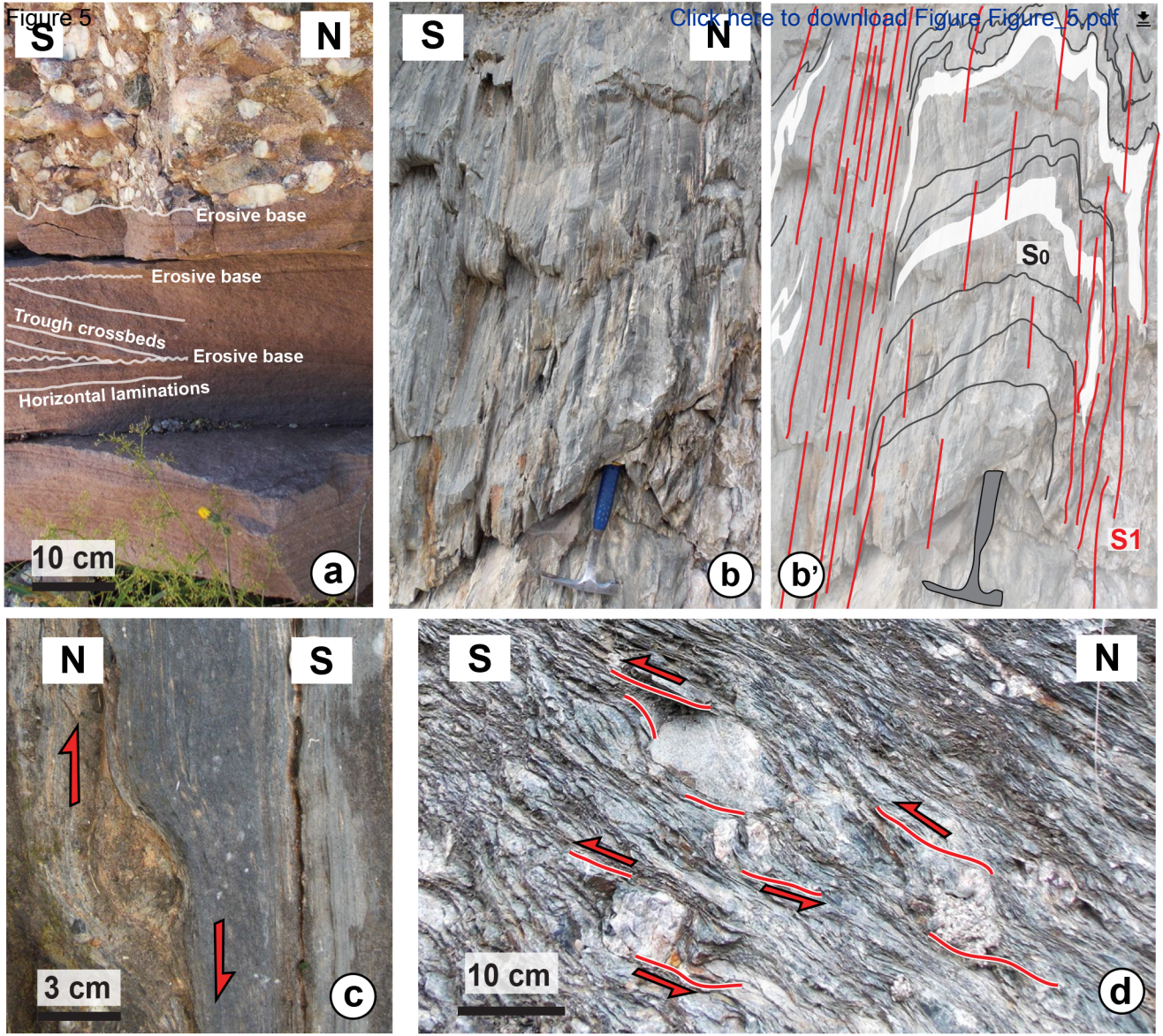

Cochelin et al., Figure 5

Figure 6

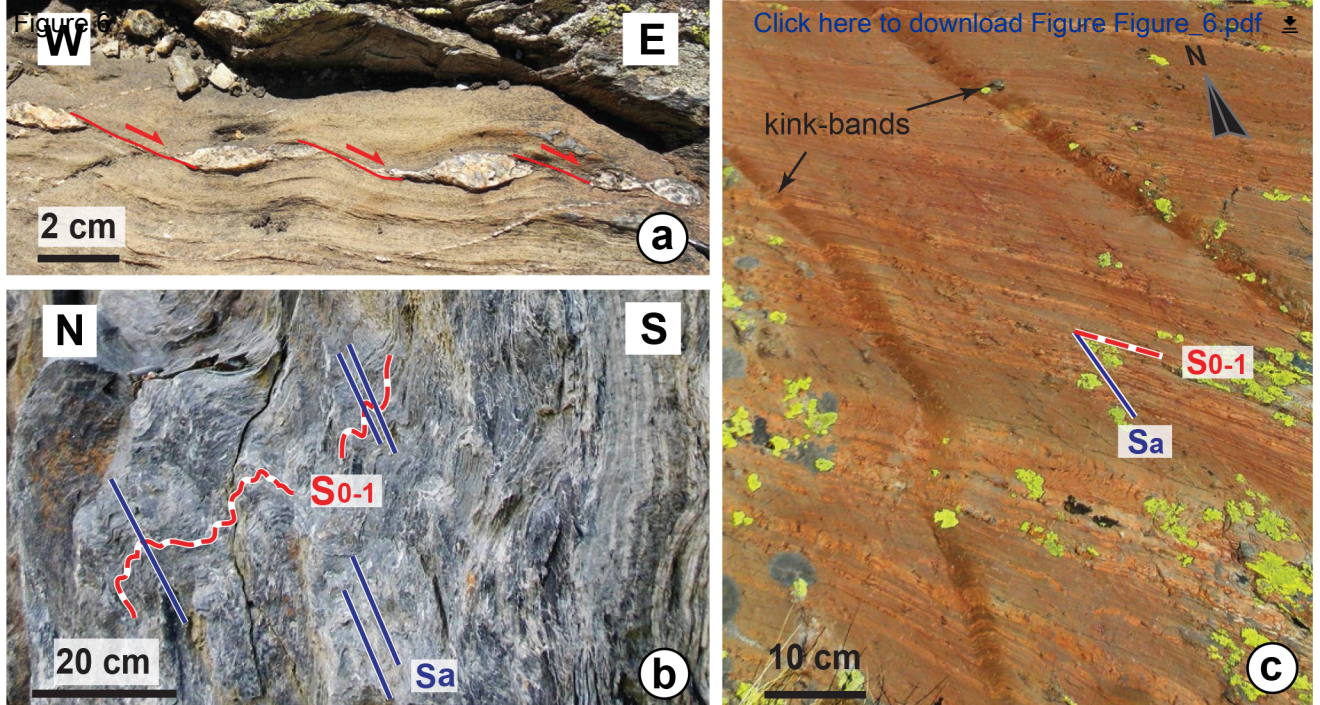

Cochelin et al., Figure 6

Figure 7

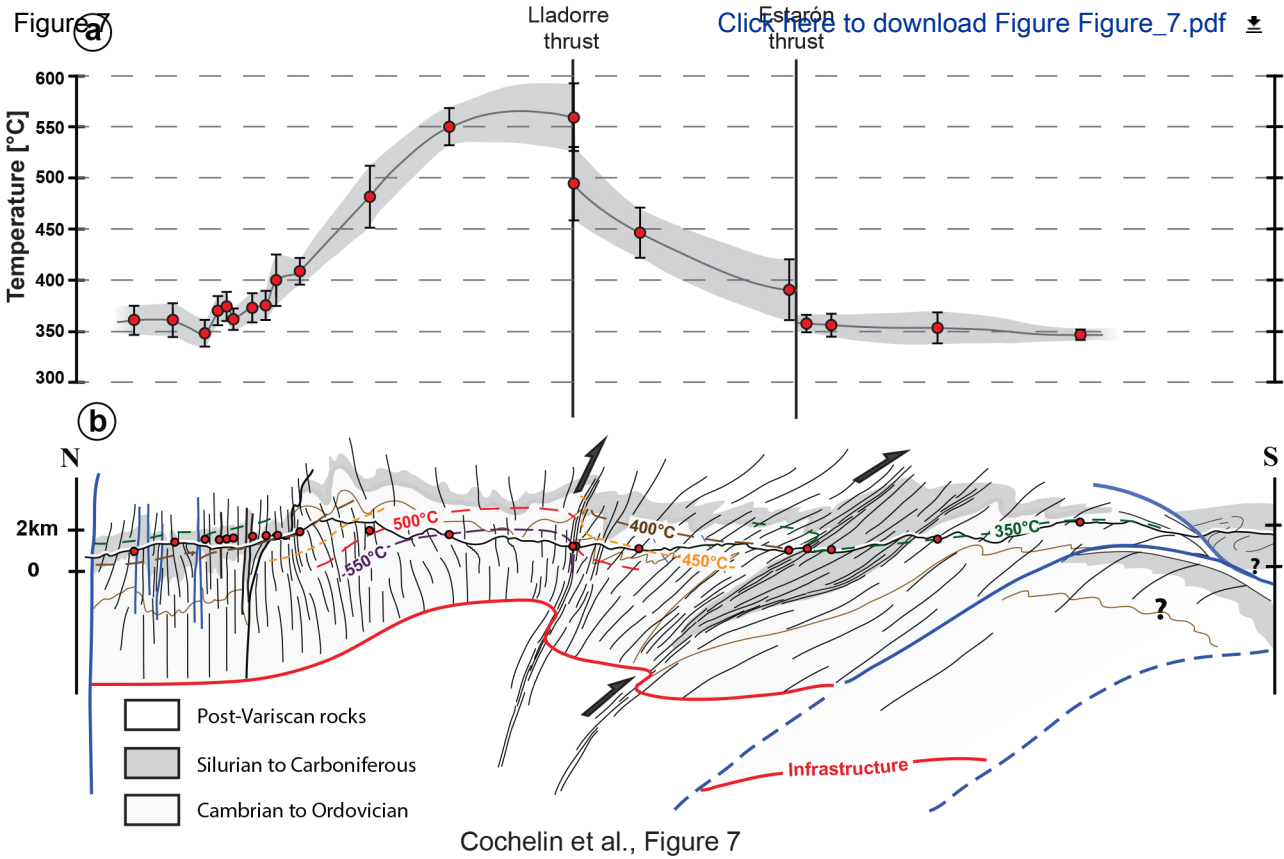

Cochelin et al., Figure 7

Figure 8

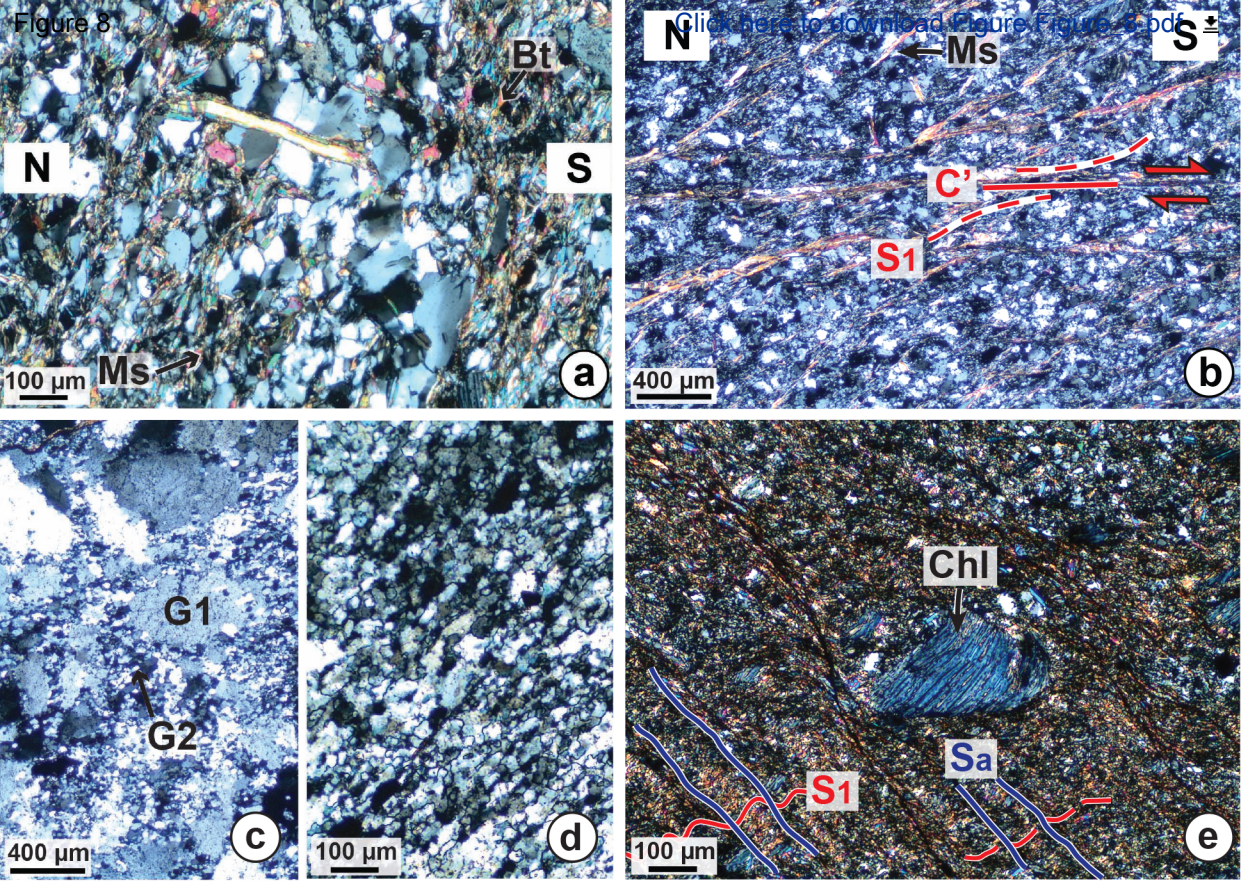

Cochelin et al., Figure 8

Figure 9

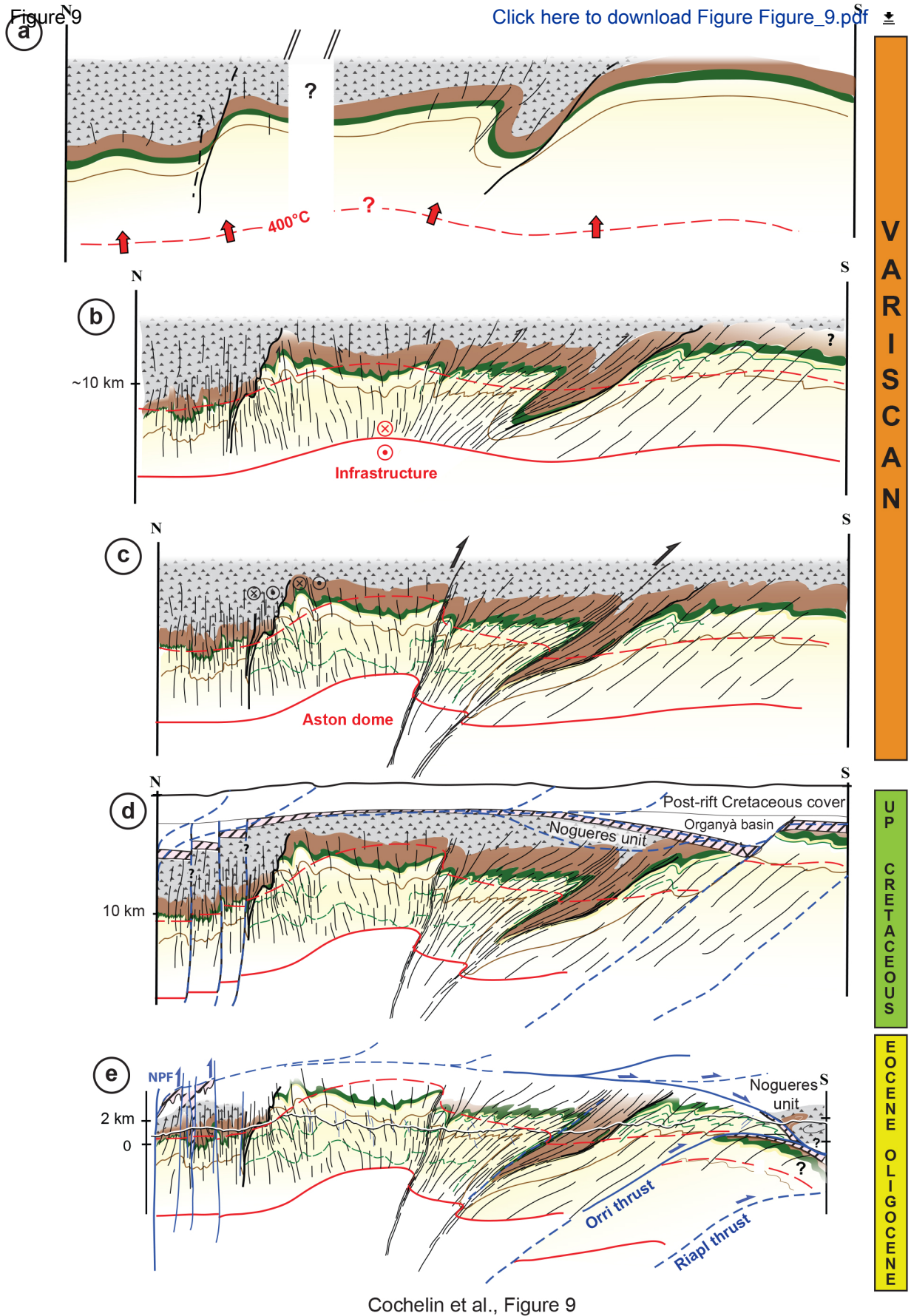

Cochelin et al., Figure 9

Figure 10

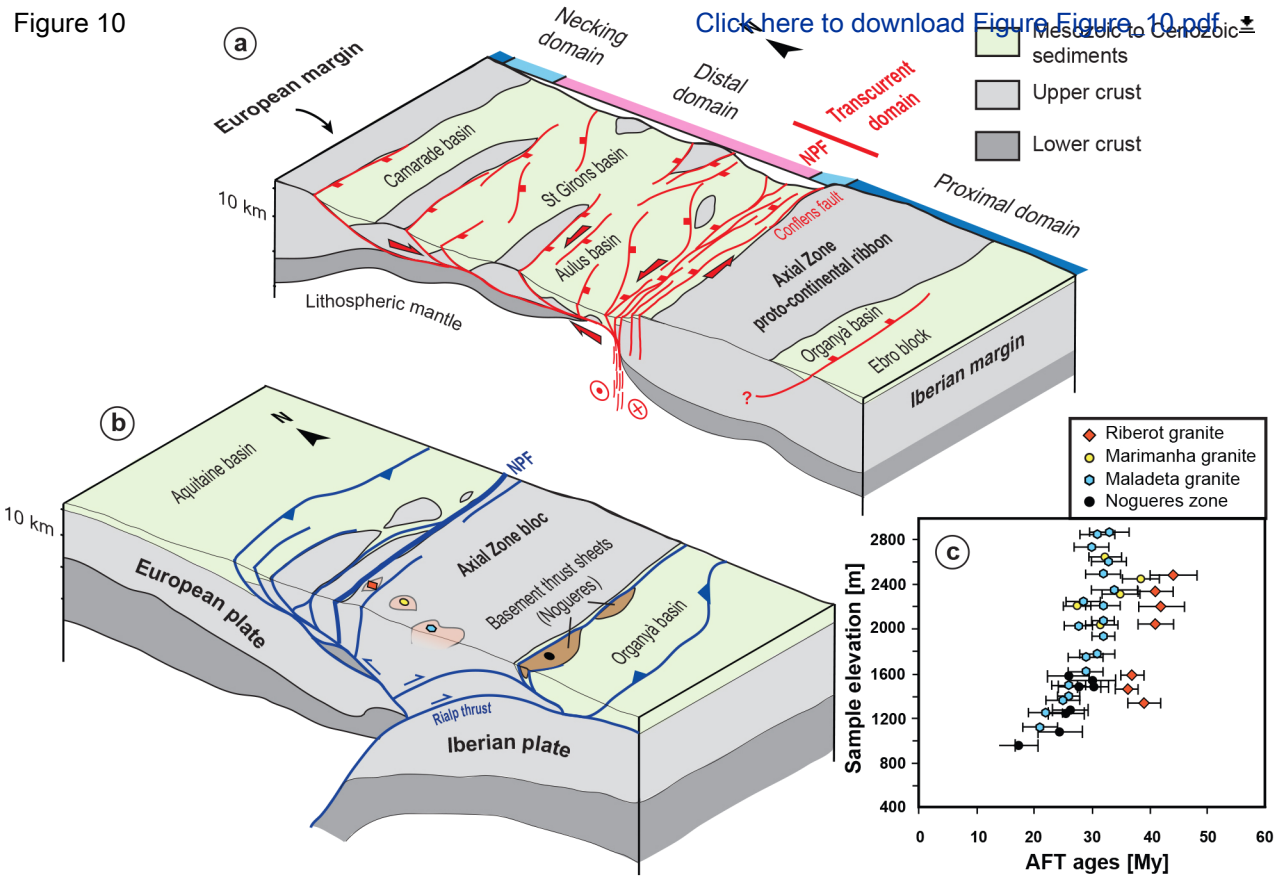

Cochelin et al., Figure 10